GAC MEDALLIST SERIES

Logan Medallist 4. Large-Scale Impact and Earth History

Richard A.F. Grieve

Department of Earth Sciences
University of Western Ontario
1151 Richmond Street, London
Ontario, N6A 5B7, Canada
Email: richard.grieve@canada.ca

SUMMARY
The current record of large-scale impact on Earth consists of close to 200 impact structures and some 30 impact events recorded in the stratigraphic record, only some of which are related to known structures. It is a preservation sample of a much larger production population, with the impact rate on Earth being higher than that of the moon. This is due to the Earth's larger physical and gravitational cross-sections, with respect to asteroidal and cometary bodies entering the inner solar system. While terrestrial impact structures have been studied as the only source of ground-truth data on impact as a planetary process, it is becoming increasingly acknowledged that large-scale impact has had its effects on the geologic history of the Earth, itself. As extremely high energy events, impacts redistribute, disrupt and reprocess target lithologies, resulting in topographic, structural and thermal anomalies in the upper crust. This has resulted in many impact structures being the source of natural resources, including some world-class examples, such as gold and uranium at Vredefort, South Africa, Ni–Cu–PGE sulphides at Sudbury, Canada and hydrocarbons from the Campeche Bank, Mexico. Large-scale impact also has the potential to disrupt the terrestrial biosphere. The most devastating known example is the evidence for the role of impact in the Cretaceous–Paleocene (K–Pg) mass extinction event and the formation of the Chicxulub structure, Mexico. It also likely had a role in other, less dramatic, climatic excursions, such as the Paleocene–Eocene–Thermal Maximum (PETM) event. The impact rate was much higher in early Earth history and, while based on reasoned speculation, it is argued that the early surface of the Hadean Earth was replete with massive impact melt pools, in place of the large multiring basins that formed on the lower gravity moon in the same time-period. These melt pools would differentiate to form more felsic upper lithologies and, thus, are a potential source for Hadean-aged zircons, without invoking more modern geodynamic scenarios. The Earth-moon system is unique in the inner solar system and currently the best working hypothesis for its origin is a planetary-scale impact with the proto-Earth, after core formation at ca. 4.43 Ga. Future large-scale impact is a low probability event but with high consequences and has the potential to create a natural disaster of proportions unequalled by other geologic processes and threaten the extended future of human civilization, itself.

RÉSUMÉ
Le bilan actuel de traces de grands impacts sur la Terre se compose de près de 200 astroblèmes et d'une trentaine d'impacts enregistrés dans la stratigraphie, dont seulement certains sont liés à des astroblèmes connus. Il s'agit d'échantillons préservés sur une population d'événements beaucoup plus importante, le taux d'impact sur Terre étant supérieur à celui de la lune. Cela tient aux plus grandes sections transversales physiques et gravitationnelles de la Terre sur la trajectoire des astéroïdes et comètes qui pénètrent le système solaire interne. Alors que les astroblèmes terrestres ont été étudiés comme étant la seule source de données avérée d'impacts en tant que processus planétaire, de plus en plus on reconnaît que les grands impacts ont eu des effets sur l'histoire géologique de la Terre. À l'instar des événements d'énergie extrême, les impacts redistribuent, perturbent et remanient les lithologies impliquées, provoquant dans la croûte terrestre supérieure des anomalies topographiques, structurelles et thermiques. Il en a résulté de nombreux astroblèmes à l'origine de ressources naturelles, dont certains exemples de classe mondiale tels que l'or et l'ura-

Geoscience Canada, v. 44, https://doi.org/10.12789/geocanj.2017.44.113 pages 1–26

nium à Vredefort en Afrique du Sud, les sulfures de Ni–Cu–PGE à Sudbury au Canada, et les hydrocarbures du Banc de Campeche au Mexique. Les grands impacts peuvent également perturber la biosphère terrestre. L'exemple le plus dévastateur connu nous est donné des indices du rôle de l'impact dans l'extinction de masse au Crétacé–Paléogène (K–Pg) et la formation de la structure de Chicxulub, au Mexique. Il a également probablement joué un rôle dans d'autres événements climatiques extraordinaires moins dramatiques, comme le Maximum thermal du Paleocène–Eocène (PETM). Le taux d'impact était beaucoup plus élevé au début de l'histoire de la Terre et, tout en étant basé sur une spéculation raisonnée, on fait valoir que la surface précoce de la Terre à l'Hadéen était tapissée de grands bassins en fusion, au lieu de grands bassins à couronnes multiples tels ceux qui se sont formés à la même période sur la lune ayant une gravité inférieure. Ces bassins en fusion se seraient différenciées pour constituer des lithologies plus felsiques sur le dessus, devenant ainsi une source potentielle de zircons d'âge Hadéen, sans qu'il soit nécessaire d'invoquer des scénarios géodynamiques plus récents. Le système Terre-lune est unique dans le système solaire interne. Actuellement la meilleure hypothèse de travail pour son origine est un impact planétaire avec la proto-Terre, après la formation du noyau à env. 4,43 Ga. La probabilité d'un futur grand impact est faible mais comporte des conséquences capables d'engendrer un désastre naturel aux proportions inégalées comparé à d'autres processus géologiques, menaçant l'avenir de la civilisation humaine elle-même.

Traduit par le Traducteur

INTRODUCTION

Planetary exploration has clearly demonstrated that impact is a ubiquitous process throughout the solar system. Impact was dominant in early planetary history and its effects are most obvious on smaller, airless bodies. For example, even a casual examination of orbital imagery of the Earth's moon clearly illustrates the importance of impact in lunar geologic history (Fig. 1a). The same can not be said for imagery of the Earth (Fig. 1b). The Earth's physical cross-section, however, is ~ 3.5 times larger than that of the moon. More importantly, from the point of view of incoming extraterrestrial bodies, its gravitational cross-section is even larger (~ 50 times larger for an average asteroidal impact velocity). Thus, the Earth has presented a much larger target to asteroidal and cometary bodies entering the inner solar system and, therefore, must have received many more impacts than the moon throughout geologic time. The simplest explanation for the apparent contradiction in the appearance of the surface of the Earth compared to that of the moon in orbital imagery lies in the fact that the results of the impact, impact structures and their attendant ejecta, are surface features. The Earth is the most active of the terrestrial, or silicate, planets in terms of endogenic geologic processes. Its surface is constantly being reworked and reshaped through tectonic, erosional and depositional processes. Through this resurfacing, the Earth's impact record has been obscured and largely removed. As a result, the Earth's known share of impact structures is not a production population, as on many areas of the moon, but is a preservation sample of an originally much larger population.

Unlike some other geologic processes, such as volcanic eruptions, earthquakes and inundation and erosional events, major terrestrial impact events have not occurred on the recorded human time-scale. Impact is also unlike other geologic processes in terms of the extreme pressures and temperatures generated and the very high strain rates and short time-scales involved. These may be among the reasons that the geoscience community was relatively late in recognizing the occurrence of terrestrial impact structures. The first terrestrial structure to be suggested as the result of impact was the now famous 1.2 km diameter Meteor or Barringer crater in Arizona, USA (Barringer 1905). Its origin was controversial and remained largely so for over 50 years, until the discovery of coesite, the high pressure polymorph of quartz, at Barringer (Chao et al. 1960). A major increase in the scientific interest into the nature of terrestrial impact structures occurred leading up to and during the Apollo missions by NASA, where they served as terrestrial analogs for lunar impact craters. It was in this period when the diagnostic effects of impact on rocks and minerals, known as shock metamorphism, were firmly established (e.g. French and Short 1968). At that time, the study of impact processes was the domain of a relatively small number of 'specialists' and impact was still generally regarded by the larger community as a significant process in the geologic history of other planetary bodies but not of particular significance to that of the Earth.

This perception remained largely in place until, initially, geochemical, and, later, physical evidence began to emerge for the role of impact in the Cretaceous–Paleogene (K–Pg) mass extinction event (e.g. Alvarez et al. 1980; Ganapathy 1980; Bohor et al. 1984). As with the initial suggestion that the Barringer crater was produced by a terrestrial impact event, this working hypothesis was not without controversy, particularly in some segments of the geoscience community. As additional and equivalent evidence for impact was forthcoming from other K–Pg boundary sites world-wide, however, the working hypothesis gained more acceptance. It received a major increase in credibility with the eventual identification of the actual K–Pg impact site, namely the buried 180 km diameter Chicxulub impact structure in the Yucatan, Mexico (Hildebrand et al. 1991). Although Chicxulub was not without its own initial controversies, e.g. its exact size and morphology, these have largely dissipated through the results of extensive geophysical, particularly, reflection seismic, campaigns (e.g. Morgan et al. 1997, 2011). In addition, there have been accompanying drilling programs by the International Continental Drilling Program (ICDP), National Autonomous University of Mexico (UNAM), and most recently the completion of a joint Integrated Ocean Drilling Program (IODP)-ICDP drilling of Chicxulub's peak-ring structure off-shore (Morgan et al. 2015, 2016). The working hypothesis relating the K–Pg boundary sites world-wide and the mass extinction to a major impact event on Earth and the ensuing debate and studies moved the perception of impact from one of it being almost exclusively a planetary process to one of also being a process of some

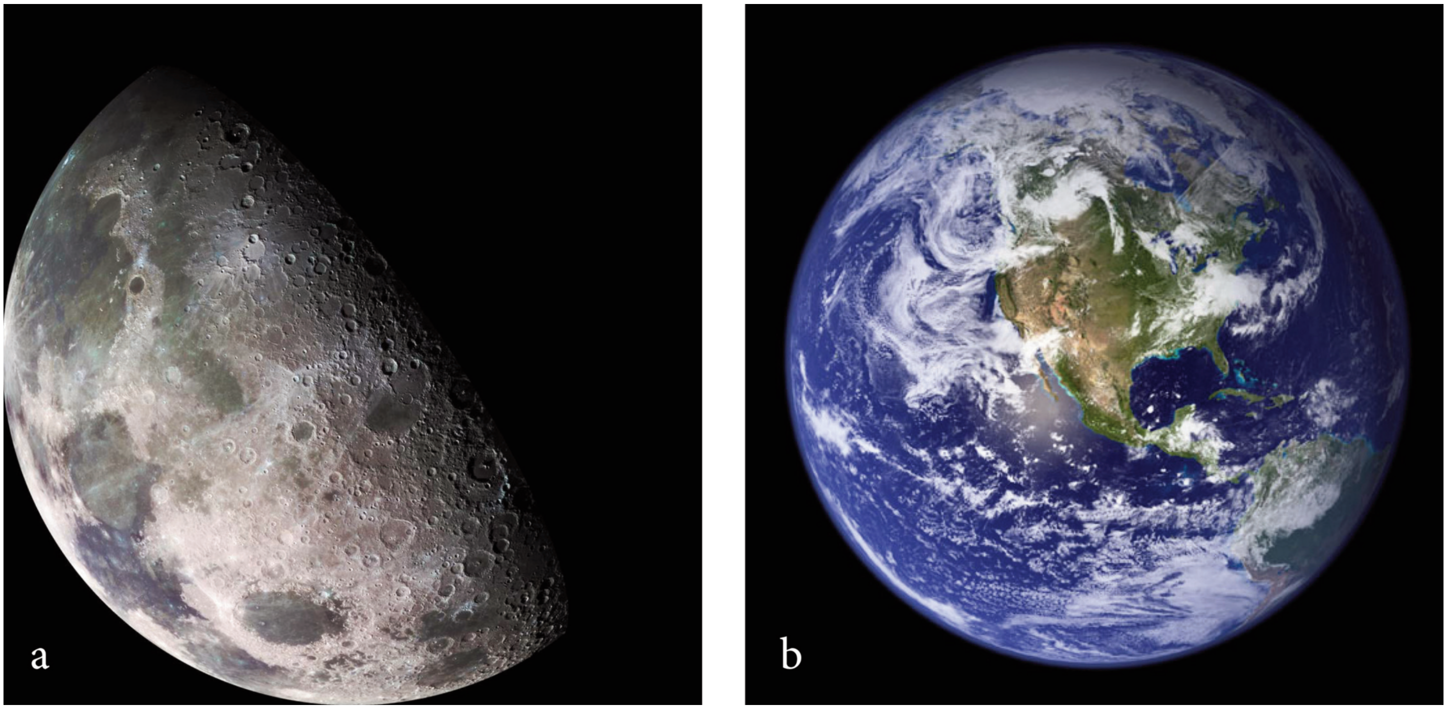

Figure 1. a) Orbital image of the moon, indicating its highly cratered surface. b) Orbital image of the Earth, indicating its apparently uncratered surface. NASA imagery.

potential importance in the context of terrestrial geologic history. It also had the effect of broadening the interest in and knowledge of impact processes to the larger, and more general, geoscience community. So much so that today, the discovery and documentation of a new terrestrial impact structure or impact event are as likely to be authored by workers from the larger geoscience community, as by those specializing in impact studies.

While the K–Pg boundary remains currently the sole example of a terrestrial mass extinction, with demonstrable evidence for the role of a major impact event on Earth, it is the thesis of this contribution that the role of large-scale impact in Earth history is much more diverse and goes well beyond this apparently singular event. As most of the terrestrial impact record has been destroyed by endogenic geologic processes, some of what is presented is based on planetary analogies and reasoned speculation.

THE TERRESTRIAL IMPACT RECORD: AN OVERVIEW

Small extra-terrestrial objects enter the Earth's atmosphere, which retards their cosmic velocity, every day and either burn-up in the atmosphere as meteors or land on Earth, at relatively low velocities, as meteorites. Larger objects ($> 9 \times 10^7$ kg), however, do not have their velocity reduced by atmospheric passage and impact the Earth with a velocity that is a combination of their cosmic velocity and the Earth's gravitational attraction. The minimum impact velocity of such objects is 11.2 $km.s^{-1}$, the escape velocity of the Earth. Asteroidal bodies are the most common of such objects and impact with an average velocity of ~ 18 $km.s^{-1}$. Less common are impacts by short-period comets, with an average impact velocity of ~ 30 $km.s^{-1}$. Long-period comets are even less common but impact with a higher average velocity of ~ 50 $km.s^{-1}$ (e.g. http://impact.ese.ic.ac.uk/ImpactEffects/).

On impact, these asteroidal and cometary bodies transfer their considerable kinetic energy to the target rocks. For example, a 1 km diameter, stony asteroidal body impacting the Earth at 18 $km.s^{-1}$ contains some 2.5×10^{20} J of kinetic energy. This essentially instantaneous energy release is of the same order as the annual release of internal energy of the entire Earth from crustal heat flow, volcanic eruptions and earthquakes. Impact events of this scale, however, occur on the million year time-scale. The impacting body transfers its kinetic energy to the target rocks via a shock wave, which propagates into the target rocks and back into the impacting body. In the target rocks, the kinetic energy of the impacting body is partitioned into kinetic energy, which sets the target rocks in motion and leads to the formation of a craterform, and into internal energy, which leads to shock metamorphic effects. Since stress can not be maintained at free surfaces (edges of the impacting body, the surface of the target rocks), rarefaction or release waves follow the propagating shock wave. The particle velocity vectors from rarefaction combine with those induced by the passage of the shock wave to produce the so-called 'cratering flow-field,' which results in the ejection of material from the upper and outer reaches of the target and downward displacement of material in the lower and central reaches of the target. The maximum radial extent of ejected and displaced materials in the target by the cratering flow-field defines the so-called transient cavity in an impact event. The transient cavity is a conceptual construct and only exists as an entity in the smallest of impacts. It is generally taken to be approximately parabolic in cross-section but, as indicated by its name, it represents an unstable situation due to gravitational

https://doi.org/10.12789/geocanj.2017.44.113

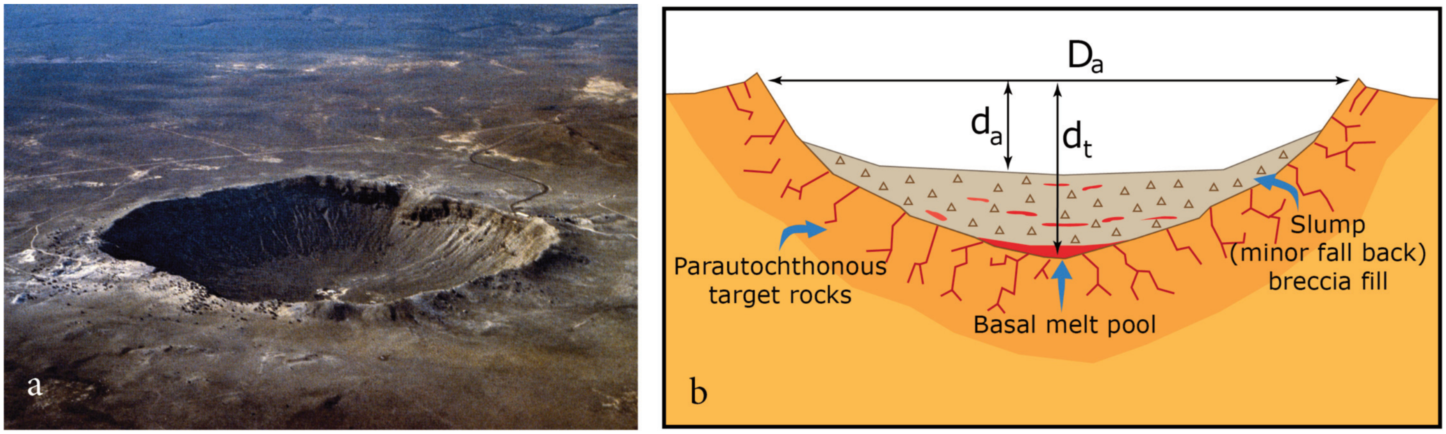

Figure 2. a) Barringer (Meteor) crater, USA, is a 1.2 km diameter (D_a) simple crater (bowl-shaped). Note rather square outline of rim, due to the effects of pre-existing regional jointing. b) Schematic cross-section of a simple crater. Note visible surface, as seen at Barringer (above), defines the apparent crater, with depth (d_a), and is underlain by a breccia lens, the base of which defines the true crater, with depth (d_t).

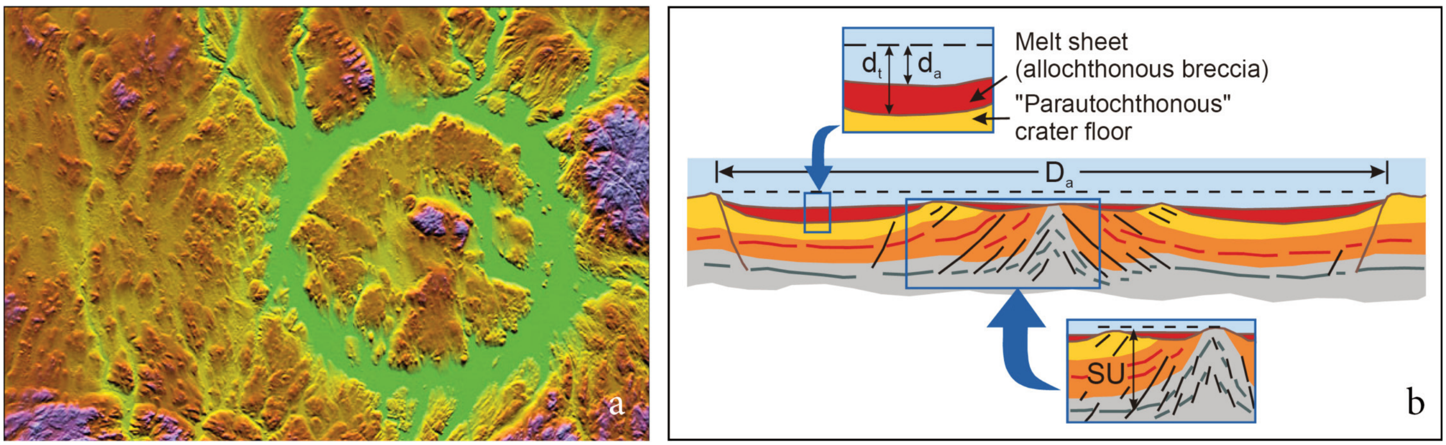

Figure 3. a) Colour image of topography of the complex Manicouagan structure, Canada, based on NASA SRTM data. Reds and blues are high, yellows and greens are low. Manicouagan has an estimated original diameter of ~ 100 km. Note the smooth annulus ~ 55 km in diameter that corresponds to the Manicouagan hydroelectricity reservoir, the slightly off-centre topographic peak (horst of uplifted anorthosite target rocks) and the topographic lineations that reflect the effects of glaciation, particularly within the annulus where the coherent impact melt sheet outcrops. b) Schematic cross-section of a complex impact structure, with a central peak and ring. Note the structural uplift (SU) of parautochthonous target rocks in the centre and that d_a and d_t are much shallower with respect to D_a, compared to a simple crater, reflecting the greater modification with respect to the initial transient cavity. As with simple crater, the interior of complex structures are partially filled with allochthonous impact lithologies (impact melt rock, breccia).

forces and collapses and is modified, almost as it forms and grows, resulting in the final craterform.

The final craterform is a function of the size of the impact event, planetary gravity and the dynamic strength of the target rocks. Smaller impact structures are so-called simple structures (Fig. 2a). When fresh, they are bowl-shaped in form, with an upraised and overturned rim, which is overlain by ejecta. They are partially filled, to approximately half the depth of the original transient cavity, with impact lithologies, such as various types of breccias and impact melt rocks (Fig. 2b). These lithologies largely represent fractured and brecciated transient cavity wall rocks and their lining that collapsed inward under gravity, during the modification of the transient cavity. Larger impact structures are so-called complex structures (Fig. 3a, b). Complex structures occur at diameters > 2–5 km on Earth, depending on the nature of the target rocks (crystalline, sedimentary or both). They are characterized by a complex, faulted and collapsed rim area, a relatively flat floor and some form of uplifted structure in the centre (Fig. 3b). They represent a much more highly modified craterform, with respect to the transient cavity, than simple structures. The uplifted central structure consists of parautochthonous target rocks from the transient cavity floor. It has the form of an emergent topographic peak or ring, above the crater-fill products lining the parautochthonous crater floor, depending on the size of the impact event. The vertical amount of this 'structural uplift' in the centre of complex structures is approximately 0.1 of the rim diameter (Fig. 4). The largest impact structures, which have an internal topographic ring structure, are often referred to as impact basins. As with simple structures, the crater-fill products at complex structures consist of various breccias and impact melt rocks, the latter being a dominant lithology in impacts into crystalline targets (Fig. 3b). The crater-fill products represent material that failed to be ejected from the transient cavity.

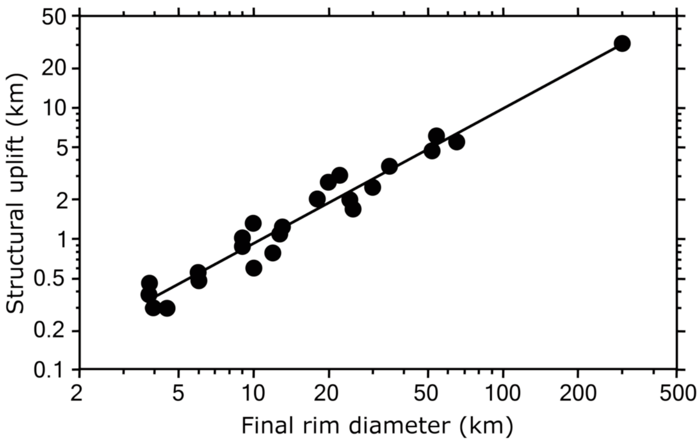

Figure 4. Logarithmic plot of apparent diameter (D_a) against structural uplift (SU) for terrestrial complex impact structures, indicating that uplift varies as ~ 0.1 D_a.

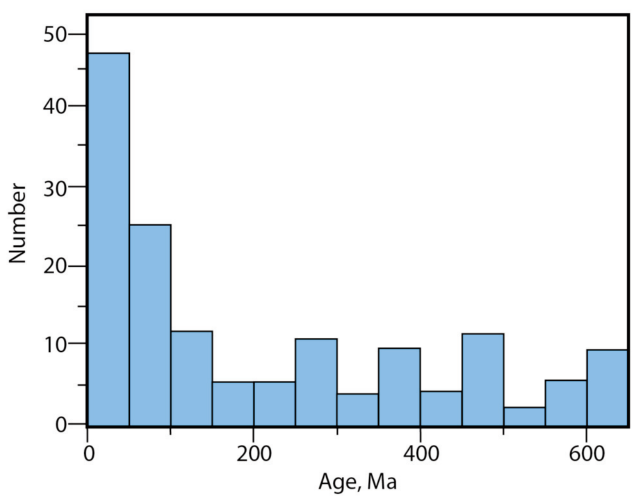

Figure 5. Histogram of the ages of Phanerozoic terrestrial impact structures, with < ± 10 m.y. age uncertainty and binned by 50 Ma. Note temporal bias towards 'young' ages, reflecting the effects of endogenic terrestrial geologic processes in removing and obscuring 'older' impact structures.

The preservation sample of impact structures that constitutes the terrestrial impact record is biased, compared to that, for example, of the moon. It is biased towards larger and younger structures (Fig. 5). This is a reflection of the fact that not only are such larger structures more likely to be preserved in the very active terrestrial geologic environment but they are also more likely to be recognized. Their spatial distribution is also biased towards the more geologically stable cratonic areas of the Earth, where they are more likely to be preserved (Fig. 6). In some cases, terrestrial impact structures have been eroded below the original crater floor and no longer have an associated negative topographic expression. In several cases, differential erosion has resulted in their present topographic expression being positive, relative to the surrounding terrain (e.g. only an erosionally resistant central structure remains). Thus, it is more appropriate, and encompassing, to refer to them as terrestrial impact 'structures' as opposed to 'craters.'

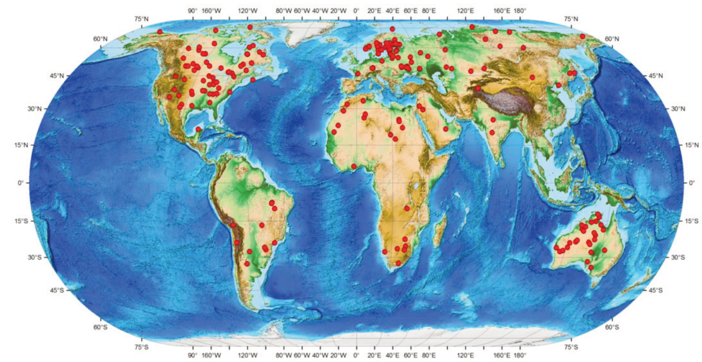

Figure 6. Spatial distribution of known terrestrial impact structures. Note bias towards preservation and recognition of impact structures on stable cratonic areas, particularly where there have been active programs to identify impact structures (e.g. North America, Fennoscandia, Australia). Image from G. Osinski, Western University.

The known terrestrial impact record currently stands at ~ 200 impact structures, with several new discoveries per year. Basic information (name, size, age, location, etc.) on known terrestrial impact structures can be found at http://www.passc.net/EarthImpactDatabase/. They range in size from metres to ~ 300 km in diameter and in age from Recent to Precambrian. Approximately 30% of known terrestrial impact structures are buried by post-impact sediments. They were detected originally as geophysical anomalies and subsequently drilled for economic or scientific purposes. In addition, there are ~ 30 impact events recorded in the stratigraphic column, in the form of ejecta deposits, spherule layers, tektites and microtektites, only some of which are related to known impact structures.

Given the effects of erosion and the very active endogenic geologic environment, the confirmation of the occurrence of a terrestrial impact structure is not based on its topographic expression, although that may be the reason for its initial interest as a potential impact structure. Confirmation of an impact origin is based on the occurrence of irreversible changes in the target rock and minerals by shock metamorphism or the physical or chemical evidence of meteoritic material. Shock metamorphic effects are a direct result of the shock wave increasing the internal energy of the target rocks and are, thus, diagnostic of impact. They do not occur below shock pressures of several GPa and continue up to pressures of 100's of GPa (Fig 7). They include the formation of: shatter cones, the only known megascopic shock effect; microscopic so-called planar deformation features (PDFs), best known in quartz and feldspar; so-called diaplectic or thetomorphic solid-state glasses in quartz and feldspar; impact melt rocks and glasses; and various high pressure polymorphs, such as coesite and stishovite from quartz and diamond from graphite (Fig. 8).

Shock metamorphic effects are not produced directly by the passage of the shock wave and compression of the target rocks but rather after the shock pressure is released, following the passage of the rarefaction wave. With increasing pressure, the net effect of shock compression and pressure release is to increase the entropy and degree of disorder in the target rocks

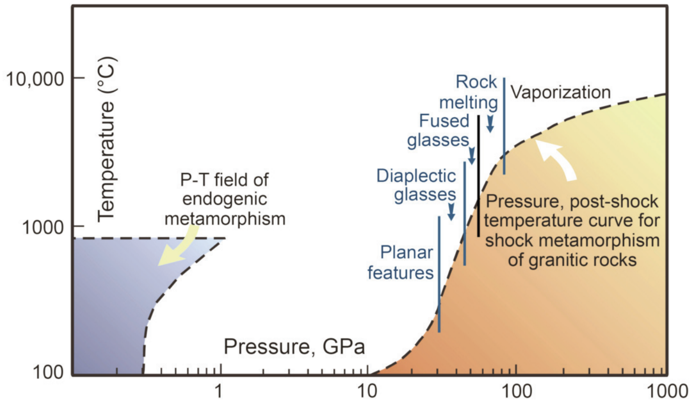

Figure 7. Logarithmic pressure–temperature curve for shock metamorphism in granitic rocks, with the attendant pressure–temperature range of some specific shock metamorphic features, compared with field of endogenic metamorphism.

and their constituent minerals, such that still crystalline shocked rocks and minerals are less dense than their original state. Impact melting (and even vaporization and ionization) occur as a result of the fact that considerable pressure–volume work is performed on the target rocks during shock compression but pressure release is adiabatic and not all this pressure–volume work is recovered. The work not recovered on pressure release is manifested as waste heat, which leads to increased post-shock temperatures and, ultimately, mineral and whole rock melting of target materials. This melting is not the same as in igneous processes and does not correspond to the standard phase diagram behaviour of rocks and minerals. It is a function of the compressibility of minerals, with more compressible minerals retaining more waste-heat and, thus, melting when subjected to lower shock pressures than less compressible minerals.

Although there are secondary effects due to target type (e.g. crystalline versus sedimentary), impact is a scale-dependent process that is very much governed by physics. The above has been the briefest of summaries regarding impact processes, and readers interested in more detail, particularly in regard to the physics behind impact cratering, are referred to Melosh (1989). Further entrance to literature can be made through a series of Geological Society of America Special Papers, based on conferences on "Large-scale impact and planetary evolution", the latest of which was edited by Osinski and Kring (2015). The most recent synopsis of current knowledge on impact process and products can also be found in Osinski and Pierazzo (2012).

The effects of large-scale impact on the Earth are discussed below, in the order of decreasing empirical evidence and increasing reasoned speculation, i.e. from the present back through the Phanerozoic to the earliest times in Earth's history, for which no substantive record remains. There is also an accompanying thematic focus. The present and historical time illustrate the economic benefits of impact to human civilization, with the focus on the observation that a number of impacts have resulted in the concentration of exploitable natural resources. The Phanerozoic geologic record highlights the potential for major impacts to affect the terrestrial biosphere, with emphasis on the working hypothesis that a major impact

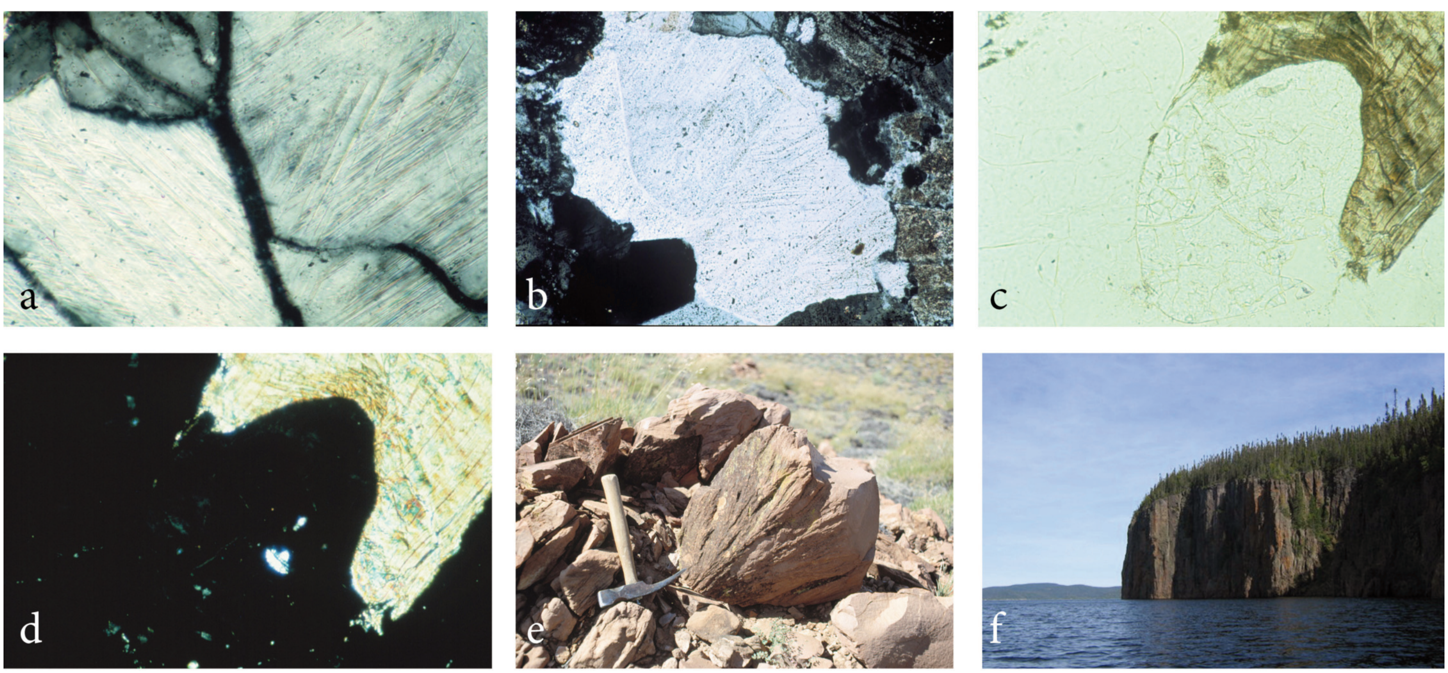

Figure 8. a) Photomicrograph of relatively fresh (undecorated) planar deformation features (PDFs) in quartz in target rocks at the 36 ± 4 Ma Mistastin structure, Canada. Crossed polars, field of view 1 mm. b) Photomicrograph of partially annealed (decorated) planar deformation features in quartz in target rocks at 1.85 Ga Sudbury structure. Crossed polars, field of view 1 mm. c) Photomicrograph of granodiorite target rocks at Mistastin structure, with quartz (white, high relief), feldspar (white, low relief) and biotite (brown). Plane light, field of view 1 mm. d) As c) but with crossed polars. Both quartz and feldspar are isotropic (black), as they are solid-state diaplectic glasses that have retained their original crystal forms. e) Shatter cones at the Gosses Bluff structure, Australia. Hammer for scale. f) Cliffs of coherent impact melt rock at the Manicouagan structure, Canada. Current thickness of melt rocks is ~ 200 m.

event was the cause of the K–Pg mass extinction event. The earliest times of Earth history are the most speculative, with respect to the effects of impact on Earth history, but some reasoned potential consequences of major impacts and their role in the earliest crustal evolution of the Earth and the formation of the Earth's moon are presented.

NATURAL RESOURCES AND IMPACT

Some 20% of known terrestrial impact structures have some form of associated natural resources and, of these, about half are being exploited or have been historically. Reimold et al. (2005) list 56 impact structures with 'economic interests,' including structures that provide sites for recreational activities and/or serve as tourist attractions. In addition, several structures have been, or are being, exploited as a source of building materials (e.g. Ries, Germany; Rochechouart, France), or sources of groundwater or as reservoirs for hydro-electric power generation (e.g. Puchezh-Katunki, Russia; Manicouagan, Canada). The economic value of such resources, however, can be considerable. For example, the electricity generated by the Manicouagan reservoir is of the order of 5000 $GWh.a^{-1}$, which is sufficient to supply a small city (~ 500,000 households with average consumption) and worth approximately $700 million per year (at 2016 Ontario electricity rates).

Natural resource deposits at terrestrial impact structures are considered under the headings of progenetic, syngenetic and epigenetic (Grieve and Masaitis 1994). Commercial accumulations of hydrocarbons at terrestrial impact structures result from a number of processes related to impact and are considered separately. Some generalities of the types of deposits are given in Table 1 and only a few examples of the larger and more important deposits are given here. For more comprehensive coverage of the full range of natural resources occurring in association with terrestrial impact structures, the reader is referred to Reimold et al. (2005) and Grieve (2012).

Progenetic Deposits

Progenetic economic deposits originated prior to the impact event by endogenic terrestrial concentration mechanisms. The impact event itself subsequently resulted in the spatial redistribution of these deposits and, in most cases, brought them to a surface or near-surface stratigraphic position, from where they can be exploited. Progenetic economic deposits in impact structures include iron, uranium, gold, hydrocarbons and others (Table 1). In many cases, the deposits are relatively small. For illustration, a Canadian (Carswell) and a world-class (Vredefort) example are presented here.

Uranium at Carswell

The Carswell structure in northern Saskatchewan, Canada, is a complex impact structure in the Athabasca Basin. The Proterozoic-aged Athabasca Basin is the richest known and second largest uranium-producing region in the world. The Carswell structure has been eroded to below the original crater floor and is apparent in Shuttle Radar Topography Mission (SRTM) imagery as two circular ridges, corresponding to the outcrop of the dolomite of the Carswell Formation (Fig. 9a, b). The outer ridge is ~ 39 km in diameter and is generally quoted as the diameter of the structure; although it may well be an underestimate. Interior to this, there is an annular trough, occupied by sandstone and conglomerate of the Athabasca Group. This trough is ~ 5 km wide and rises to a core, ~ 20 km in diameter, of mixed gneisses of the basement, which are believed to have been structurally uplifted by > 2 km (Baudemont and Fedorowich 1996). The inner contact of the Athabasca Group sedimentary rocks with the basement is faulted and truncated in places and offset by radial faults. The outcrops of the sedimentary rocks are unique to the area and owe their preservation to having been down-faulted > 1 km in the impact. Brecciation is common at Carswell and affects all lithologies. So-called 'Cluff Breccias,' after exposures near Cluff Lake, include autochthonous monomict, allochthonous polymict clastic and melt-bearing breccias, as well as clast-rich impact melt rocks.

The known commercial uranium deposits (Fig. 9) occur in two main settings: at the unconformity between the Athabasca Group and the uplifted crystalline basement core, and in mylonites and along faults in the crystalline core. These deposits had grades from 0.3 to > 4% uranium oxide (Jefferson and Delaney 2007). The original uranium mineralization in the Athabasca Basin, and at Carswell, occurred during regolith development in the Precambrian, with later remobilization due to hydrothermal activity (Lainé et al. 1985). The original commercial uranium deposit discovered at Carswell, the Cluff Lake D deposit, was, at the time of mining, the richest known uranium ore body in the world. It closed in 2002, having produced 28.1 kt of 'yellow cake,' an intermediate milling product consisting mostly of uranium oxide, over its 22 year lifetime.

Baudemont and Fedorowich (1996) recognized four episodes of deformation at Carswell, with the third episode related to mineralization and the final episode related to the impact event. They noted that Carswell-related deformation reactivated earlier faults, associated with the main mineralization, and that the association was "striking". It is not clear to what extent the Carswell impact event was involved in remobilizing the uranium ores, beyond physical movement related to structural uplift. The basement-hosted ores are all associated with extensive regional alteration and hydrothermal fluid movement. All known commercial uranium deposits within the Carswell structure are currently closed. There are, however, active exploration targets, including reactivated faults, with pseudotachylitic breccia and/or 'Cluff Breccias' and uranium mineralization. In addition to bringing ore bodies to the surface, Carswell serves as a unique window into the nature of basement beneath the Athabasca Basin and, as such, serves as a guide to uranium exploration through out the entire basin.

Gold and Uranium at Vredefort

The Vredefort impact structure, South Africa (Fig. 10a, b) consists of a 44 km diameter uplifted central core of predominantly Archaean granitic gneisses, surrounded by an 18 km wide collar of steeply dipping to overturned Proterozoic sedimentary and volcanic rocks of the Witwatersrand and Ventersdrop Supergroup. This, in turn, is surrounded by a 28 km wide

https://doi.org/10.12789/geocanj.2017.44.113

Table 1. Natural Resources at Terrestrial Impact Structures.

Crater Name	Lat.	Long.	Country	Apparent Diameter (km)	Age (Ma)	Resource
Ames	36°15'N	98°12'W	USA	16	470 ± 30	Hydrocarbons
Avak	71°15'N	156°38'W	USA	14	< 95	Hydrocarbons
Boltysh	48°45'N	32°10'E	Ukraine	24	65.2 ± 0.6	Oil shale
Calvin	41°50'N	85°52'W	USA	8.5	450 ± 10	Hydrocarbons
Carswell	58°27'N	109°30'W	Canada	39	115 ± 10	Uranium
Charlevoix	47°32'N	70°18'W	Canada	54	342 ± 15	Ilmenite
Chesapeake Bay	37°37'N	76°01'W	USA	80	35.5 ± 0.3	Groundwater
Cloud Creek	43°10.6'N	106°42.5'W	USA	7	190 ± 20	Hydrocarbons
Crooked Creek	37°50'N	91°23'W	USA	7	320 ± 80	Pb–ZnPb–ZnPb–Zn
Decaturville	37°54'N	92°43'W	USA	6	< 300	Pb–Zn
Dellen	61°48'N	16°48'E	Sweden	19	89.0 ± 2.7	Hydroelectric
Kara	69°06'N	64°09'E	Russia	65	70.3 ± 2.2	Impact diamonds
Kentland	40°45'N	87°24'W	USA	13	< 97	Pb–Zn
Lonar	19°58'N	76°31'E	India	1.8	0.05 ± 0.01	Trona
Manicouagan	51°23'N	68°42'W	Canada	100	214 ± 1	Hydroelectric
Marquez Dome	31°17'N	96°18'W	USA	13	58 ± 2	Hydrocarbons
Newporte	48°58'N	101°58'W	USA	3.2	< 500	Hydrocarbons
Obolon	49°35'N	32°55'E	Ukraine	20	169 ± 7	Oil shale
Popigai	71°39'N	111°11'E	Russia	100	35.7 ± 0.2	Impact diamonds
Puchezh-Katunki	56°58'N	43°43'E	Russia	40	167 ± 3	Impact diamonds
Red Wing Creek	47°36'N	103°33'W	USA	9	200 ± 25	Hydrocarbons
Ries	48°53'N	10°37'E	Germany	24	15.1 ± 0.1	Impact diamonds; bentonite; lignite; building stone
Rochechouart	45°50'N	00°56'E	France	23	201 ± 2	Building stone
Rotmistrovka	49°00'N	32°00'E	Ukraine	2.7	120 ± 10	Oil shale
Saint Martin	51°47'N	98°32'W	Canada	40	220 ± 32	Anhydrite; Gypsum
Serpent Mound	39°02'N	83°24'W	USA	8	< 320	Pb–Zn
Sierra Madera	30°36'N	102°55'	USA	13	< 100	Hydrocarbons
Siljan	61°02'N	14°52'E	Sweden	65	362 ± 1	Pb–Zn
Steen River	59°30'N	117°30'W	Canada	25	91 ± 7	Hydrocarbons
Sudbury	46°36'N	81°11'W	Canada	150–200	1850 ± 3	Ni, Cu, PGE; Cu–Pb–Zn; Impact diamonds
Ternovka	49°01'N	33°05'E	Ukraine	11	280 ± 10	Iron; uranium; impact diamonds
Tswaing	25°24'S	28°05'E	S. Africa	1.13	0.22 ± 0.05	Trona
Viewfield	49°35'N	103°04'W	Canada	2.5	190 ± 20	Hydrocarbons
Vredefort	27°00'N	27°30'E	S. Africa	250–300	2023 ± 4	Gold; uranium
Zapadnaya	49°44'N	29°00'E	Ukraine	3.2	165 ± 5	Impact diamonds

outer broad synclinorium of gently dipping Proterozoic sedimentary and volcanic rocks of the Transvaal Supergroup. Younger sandstone and shale of the Karoo Supergroup cover the southeastern portion of the structure (Fig. 10a). The most comprehensive and recent guide to the geology of Vredefort can be found in Gibson and Reimold (2008). The Vredefort impact event occurred at 2023 ± 4 Ma (Kamo et al. 1996). Based on the spatial distribution of impact-related deformation and structural features, Therriault et al. (1997) derived a self-consistent, empirical estimate of 225–300 km for the original apparent diameter of Vredefort. A similar size estimate was derived by Henkel and Reimold (1998) and Grieve et al. (2008). These estimates effectively equate the Vredefort impact structure to the entire Witwatersrand Basin in South Africa.

The Witwatersrand Basin is the world's largest goldfield, having supplied over 40% of the gold ever mined. Since gold was discovered there in 1886, it has produced 47 kt of gold (Robb and Robb 1998). In 1970, Witwatersrand gold accounted for 80% of world's gold supply. Production has declined since, with production for 2002 ~ 350 t, or ~ 13.5% of the global gold supply. Current production accounts for < 5% of the global supply, due to the high cost of 'deep' mining, although current reserve estimates are around 20 kt of gold. Approximately 150,000 t of uranium have been mined, gener-

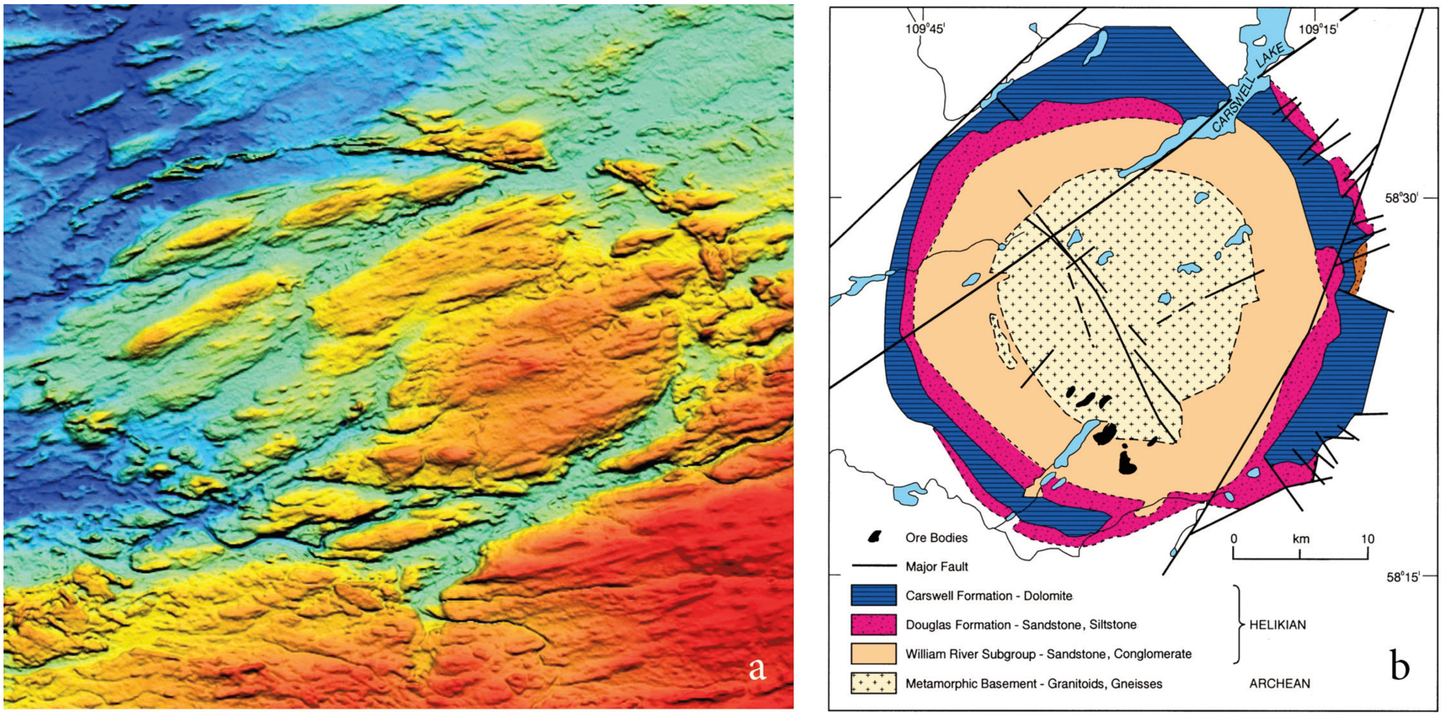

Figure 9. a) Colour image of topography of the complex Carswell structure, Canada, based on NASA SRTM data. Reds and yellows are high, blues and greens are low. Note conspicuous ridge at 39 km diameter, corresponding to the outcrop of the Carswell Formation and generally taken as the apparent diameter. Also visible are lineations in the central crystalline core due to the effects of glaciation. b) Simplified bedrock geologic map of the Carswell structure, showing uplifted crystalline core and down-faulted annulus of Carswell and Douglas Formations and the location of major uranium ore bodies.

ally as a by-product of gold mining, with estimated reserves of 475 kt (Reimold et al. 2005). Independent of impact studies, structural analyses have identified a series of concentric anticlinal and synclinal structures related to Vredefort (Fig. 10b). These Vredefort-related structures have led to the preservation of sedimentary rocks of the Witwatersrand Supergroup from erosion (McCarthy et al. 1990). The bulk of the gold has been mined from the upper succession of the Witwatersrand Supergroup known as the Central Rand Group.

General gold distribution is controlled by sedimentary attributes of the Central Rand. Pure detrital and hydrothermal models and combinations of the two have been proposed for the origin of the gold (e.g. Frimmel et al. 2005; Hayward et al. 2005; Meier et al. 2009), with clear detrital morphological features occurring with secondary, remobilized gold. This suggests that detrital gold was introduced into the basin but that some gold was subsequently remobilized by hydrothermal activity (e.g. Zhao et al. 2006). Two thermal or metamorphic events affected the rocks of the basin. A regional amphibolite facies metamorphism predates the Vredefort impact event. A later low-pressure (0.2–0.3 GPa), immediately post-impact event, however, produced peak temperatures of 350 ± 50°C in the Witwatersrand Supergroup to > 700°C in the centre of the crystalline core at Vredefort. This post-impact metamorphic-hydrothermal activity is directly attributed to the combination of post-shock heating and the structural uplift of originally relatively deep-seated parautochthonous rocks, during the Vredefort impact event (Gibson et al. 1998). Reimold et al. (1999) applied the term 'autometasomatism' to describe the alteration associated with the hydrothermal activity. This activity remobilized the gold (and uranium) within impact-related structures and fractures, which provided channels for fluid migration. A more detailed discussion of the effect of Vredefort-related hydrothermal activity can be found in Reimold et al. (2005). It is likely, however, that the Vredefort impact event played a larger role in the genesis of Witwatersrand Basin gold fields than simply preserving them from erosion by impact-related structural modification (Tucker et al. 2016).

Syngenetic Deposits

Syngenetic deposits originate as a direct result of impact processes. They owe their origin to the very high levels of impact energy deposition in the local upper crustal environment, resulting in such phenomena as phase changes and impact melting. In recent years, there has been greater recognition of the role for post-impact hydrothermal activity at impact structures (e.g. Abramov and Kring 2004; Ames et al. 2006). Post-impact hydrothermal deposits are a result of localized heating due to the impact process and, thus, considered as syngenetic deposits. The remobilization of some progenetic deposits by post-impact hydrothermal activity has blurred, in some cases, the separation between progenetic and syngenetic deposits. Syngenetic economic natural resources at impact structures include impact diamonds, Cu–Ni and platinum group sulphides and other metals (Table 1).

Impact Diamonds

The first indication of impact diamonds was the discovery in the 1960's of diamond with lonsdaleite, a high-pressure polymorph of carbon, in placer deposits (e.g. in the Ukraine),

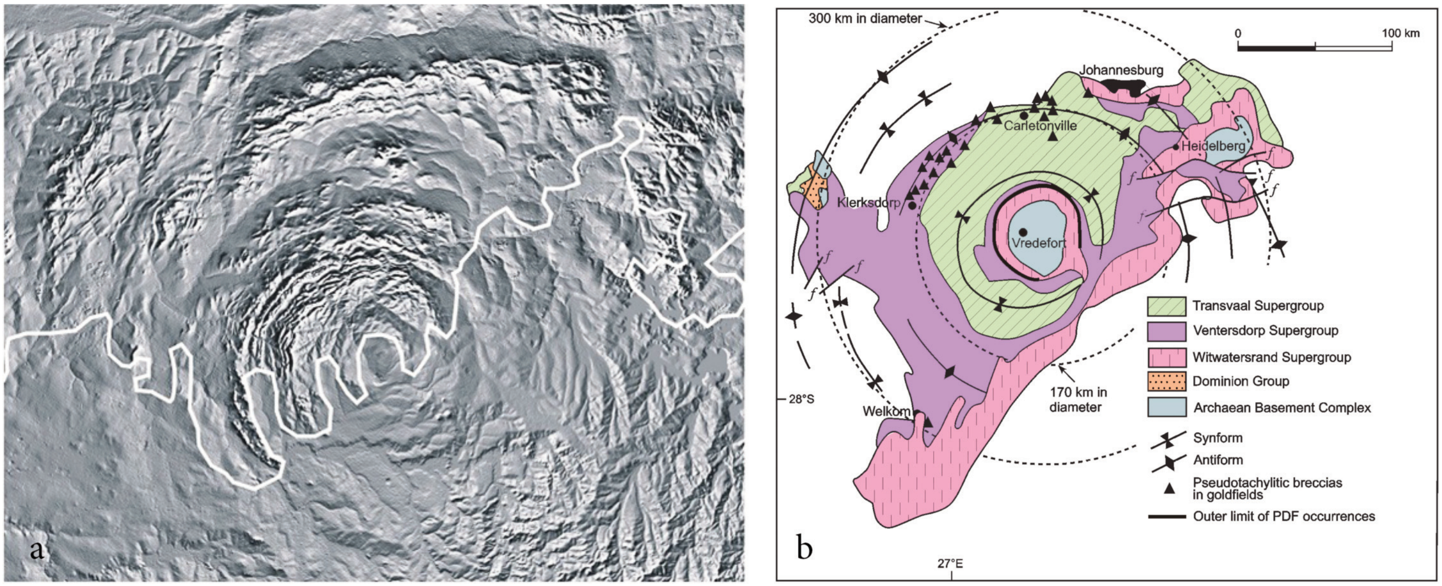

Figure 10. a) Greyscale image of topography of the complex Vredefort structure, South Africa, based on NASA SRTM. Image has been illuminated from the centre to emphasize the circumscribing anticlinal and synclinal structures. Such structures are not evident in SE quadrant, due to covering of post-impact Karoo sedimentary and volcanic rocks, 'northerly' outcrop limit of which is outlined by white line. b) Schematic geologic map of Vredefort structure, with post-impact Karoo rocks removed. Goldfields form the so-called 'golden arch,' passing through or close to Heidelberg, Johannesburg, Carletonville, Klerksdorp and Welkom.

although their source was unknown at the time. In the 1970's, diamond with lonsdaleite was discovered in the impact lithologies at the Popigai impact structure in Siberia, Russia. Since then, impact diamonds have been reported at a number of structures; e.g. Kara and Puchezh-Katunki in Russia, Lappajärvi in Finland, Ries in Germany, Sudbury in Canada, Ternovka and Zapadnaya in Ukraine and others. Impact diamonds originate when precursor carbonaceous materials (e.g. graphite, coal) are subjected to shock pressures greater than 35 GPa (Masaitis 1998). Diamonds from graphite occur as paramorphs and as microcrystalline aggregates. For example, at Popigai, these aggregates can reach 10 mm, but most are 0.2–5 mm in size (Masaitis 1998), and consist of cubic diamond and lonsdaleite. Diamonds are most common as inclusions in impact melt rocks and glass clasts in melt-bearing breccias. In impact melt rocks, diamonds occur in relatively minor amounts, with provisional average estimates in the order of 10 ppb; although, the cumulative volumes can be enormous. While still classified, the cumulative amount of impact diamonds occurring at Popigai makes it most likely the largest diamond deposit in the world. Diamonds produced by the shock transformation of graphite tend to be harder and more resistant to breaking than normal cubic diamonds. Impact diamonds, however, are not currently exploited commercially, due to the industrial production of synthetic diamonds.

Cu–Ni Sulphides and Platinum Group (PGE) Metals at Sudbury

The Sudbury structure, Ontario, Canada is the site of world-class Ni–Cu and PGE metal ores and is Canada's principal mining district. The pre-mining resources associated with the Sudbury Igneous Complex (SIC) are estimated at over 1.5 × 10^9 t of 1.2% Ni, 1.1% Cu and 1 $g.t^{-1}$ combined Pd + Pt (Farrow and Lightfoot 2002). There are also hydrothermal Zn–Pb deposits above the SIC (Ames and Farrow 2007). Nickel sulphides were first noted at Sudbury in 1856. It was not until they were 'rediscovered' during the building of the Trans-Canada railway in 1883, however, that they received attention, with the first production occurring in 1886 (Naldrett 2003). The cumulative total worth of metals produced from Sudbury is estimated at > US$300 billion (Ames and Farrow 2007).

The most prominent feature of the Sudbury structure is the ~ 30 × 60 km elliptical basin formed by the outcrop of the SIC, the interior of which is known as the Sudbury Basin (Fig. 11a, b). Neither the SIC nor the Sudbury Basin, however, is synonymous with the considerably larger Sudbury impact structure. The Sudbury impact structure includes the Sudbury Basin, the SIC and the surrounding brecciated basement rocks and covers a present area > 15,000 km^2. From the spatial distribution of shock metamorphic features (e.g. shatter cones) and other impact-related attributes, and by comparison with equivalent features at other large terrestrial impact structures (Chicxulub and Vredefort), Grieve et al. (2008) estimated that the original crater rim diameter was 150–200 km. Even larger original diameters have been suggested (e.g. Tuchscherer and Spray 2002; Naldrett 2003). With the post-impact tectonic deformation and the considerable erosion, estimated to be ~ 5–10 km, which has taken place at the Sudbury impact structure, it is difficult to constrain its original form. From its estimated original dimensions, it was most likely a peak-ring or a multiring basin (Stöffler et al. 1994; Grieve et al. 2008). Details of the geology of the Sudbury area can be found in Dressler (1984) and, most recently, in Ames et al. (2008).

The SIC is the remnant of the coherent impact melt sheet at the Sudbury structure (Grieve et al. 1991). It differs from most other terrestrial coherent impact melt sheets in that it is differentiated (due to its ~ 2.5 km thickness) and it is relatively, but not completely, clast free. For example, there are rare

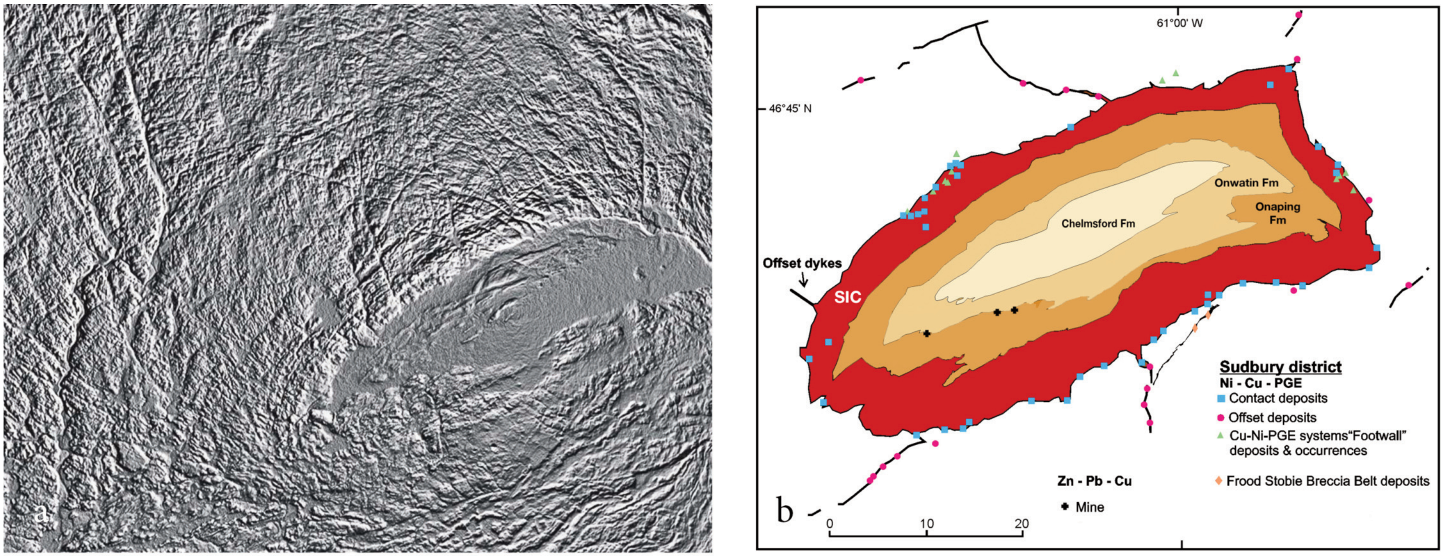

Figure 11. a) Greyscale image of topography of the complex Sudbury structure, Canada, based on NASA SRTM. Image has been illuminated from the centre. The most evident feature is the elliptical trace of the Sudbury Igneous Complex (SIC) (particularly in the north and east) and the interior Sudbury Basin. b) Simplified geologic map of ore occurrences at the Sudbury structure, relative to the SIC and overlying post-impact sedimentary rocks.

quartz clasts with partially annealed PDFs (Therriault et al. 2002). The details of the mineralogy and geochemistry support a cogenetic source for the sub-units of the so-called Main Mass of the SIC, produced by fractional crystallization of a single batch of silicate liquid (e.g. Lightfoot et al. 1997; Warner et al. 1998; Therriault et al. 2002). The conclusion that the SIC and its ores are crustal in composition is borne out by isotopic studies (e.g. Faggart et al. 1985; Walker et al. 1991; Dickin et al. 1992, 1996; Cohen et al. 2000). Osmium isotope studies of sulphides from several mines have confirmed their crustal origin from a binary mixture of Superior Province and Huronian metasedimentary target rocks (Morgan et al. 2002).

Recently, Farrow and Lightfoot (2002) and Ames and Farrow (2007) reviewed the nature of the ore deposits at Sudbury (Fig. 11b) and placed their formation in an integrated time-sequence model. They recognized: Ni–Cu–Co 'Contact' deposits associated with embayments at the base of the SIC and hosted by so-called Sublayer and Footwall Breccia; Ni–Cu–Pt–Pd–Au 'Offset' deposits associated with discontinuities and variations in thickness in the so-called Offset Dikes; and Cu–Pt–Pd–Au-rich 'Footwall' deposits that can occur in the underlying target rock, up to 1 km away from the SIC (Fig. 11). They also recognize a fourth deposit environment associated with pseudotachylitic, so-called, Sudbury Breccia. For example, the Frood-Stobie deposit, which contained some 15% of the entire known Sudbury resources and produced 600×10^6 t of ore, is hosted largely in Sudbury Breccia (Scott and Spray 2000).

The Contact deposits consist of massive sulphides and are volumetrically the largest deposit type, hosting approximately 50% of the known ore resources. The main economic Offset environments include the Copper Cliff and Worthington Offsets in the South Range, which, along with the Frood-Stobie, contain approximately 40% of the known ores at Sudbury. The Cu–PGE-rich Footwall deposits are volumetrically small (~ 10% of known ore) relative to the Contact deposits but are extremely valuable bodies, as they are relatively enriched in PGEs, in addition to copper. They represent a relatively new ore environment, which is hosted in the brecciated Footwall of the SIC and are best known in the North Range, where they occur as complex vein networks of sulphide and low sulphide, high precious metal disseminations (Ames and Farrow 2007). These Footwall deposits are the focus of much of the current exploration activity at Sudbury. There is increasing realization that hydrothermal remobilization played a role in the genesis of the Footwall deposits (e.g. Molnár et al. 2001; Hanley et al. 2005; Ames and Farrow 2007). This is consistent with the growing acknowledgement of post-impact hydrothermal activity, driven by the 'local' crustal thermal anomaly that results from large impact events (e.g. Abramov and Kring 2004).

The recent work at Sudbury can mostly be fitted into the framework of the formation of an approximately 150–200 km impact basin at 1.85 Ga. This resulted in massive (> 10^4 km^3) crustal melting producing a superheated melt of an unusual composition, which produced immiscible sulphides, during fractional crystallization. These sulphides settled gravitationally, resulting ultimately in the present Contact and Offset ore deposits. Complicating factors, but essential components of the evolutionary history of Sudbury, are the creation of a 'localized' but regional-scale impact-related hydrothermal system, which resulted in some ore fractionation and redistribution into the brecciated Footwall rocks, and the deformation by the Penokean orogeny that took place shortly after the impact. The Zn–Pb–Cu ores in the post-impact sedimentary rocks overlying the SIC are the result of the hydrothermal system fuelled by the heat of the SIC (Ames et al. 2006; Ames and Farrow 2007). This upper hydrothermal system involved sea water, as opposed to the Cl-rich brines that played a role in the origin of the Footwall deposits at the base of the SIC (Ames and Farrow 2007).

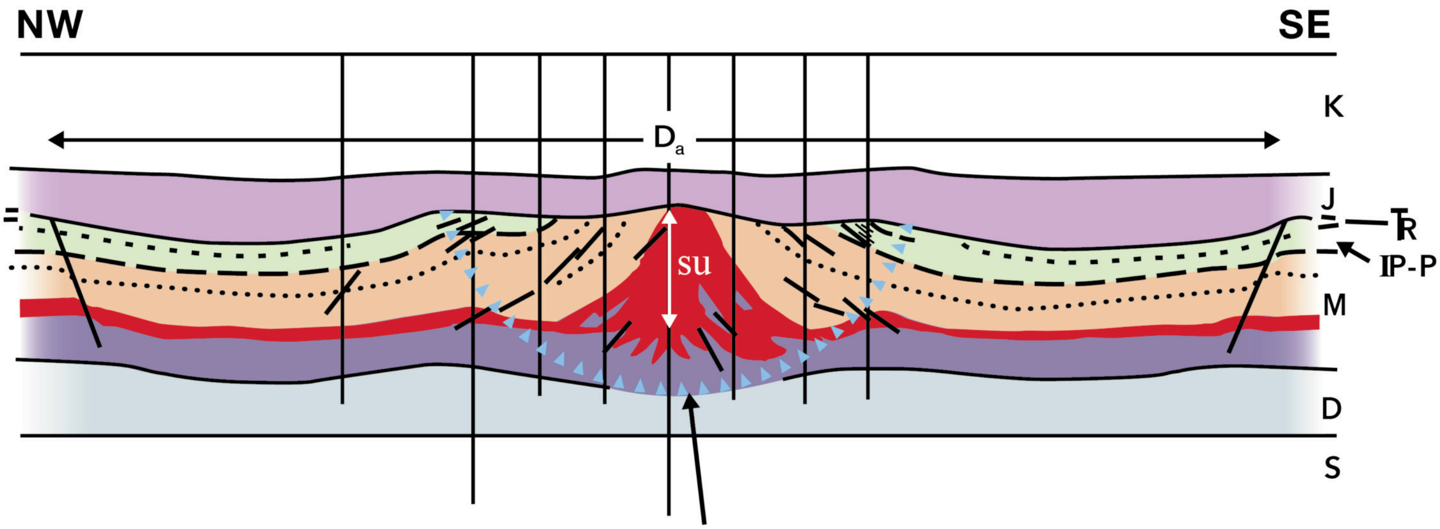

Figure 12. Schematic cross-section (no vertical exaggeration) of the complex Red Wing structure, USA. Strata: S, Silurian; D, Devonian; M, Carboniferous (Mississippian); IP-P, Permian; TR, Triassic; J, Jurassic; K, Cretaceous. Hydrocarbon production is from the duplicated, faulted and brecciated Mississippian (red) in the central structural uplift. Note difference in thickness of Mississippian in the central structural uplift, compared to annular trough and outside the structure.

Epigenetic Deposits

Epigenetic deposits result from impact producing isolated, enclosed topographic basins, with restricted sedimentation and/or the long-term flow of fluids into structural traps. Such deposits may originate almost immediately or over an extended period after the impact event and include reservoirs of liquid and gaseous hydrocarbons. There are also oil shales, various organic and chemical sedimentary rocks, as well as flows of fresh and mineralized waters (Table 1). For example, oil shales are known at Boltysh, Obolon and Rotmistrovka in the Ukraine. The most significant reserves are at Boltysh, where there is an estimated 4.5×10^9 t of oil shales, as the result of biological activity involving algae in this isolated topographic basin. A more complete listing of epigenetic deposits can be found in Reimold et al. (2005).

Hydrocarbon Accumulations

Hydrocarbons occur at a number of impact structures (Table 1). In North America, approximately 50% of the known impact structures in hydrocarbon-bearing sedimentary basins have commercial oil and/or gas fields. For example, the 25 km diameter Steen River structure in Alberta, Canada, has produced 3.5 million barrels of oil and 48.5 billion cubic feet of gas from wells on its rim, with an estimated 1.9 million barrels of oil and 4.5 billion cubic feet of gas as recoverable reserves. Oil and gas are produced from beneath the ~ 13 km diameter Marquez and Sierra Madera structures in Texas, USA (Donofrio 1998), which have a combined estimated reserve of 280 billion cubic feet of gas. Viewfield in Saskatchewan, Canada (Sawatzky 1977), which is a 2.5 km diameter simple bowl-shaped crater, produces some 600 barrels of oil and 250 million cubic feet of gas per day, with recoverable reserves estimated to be 2–4 million barrels of oil (Donofrio 1998). Some examples in which commercial hydrocarbons have accumulated under differing impact-related circumstances are given below.

Red Wing Creek

At the Red Wing Creek structure in North Dakota, USA, hydrocarbons are recovered from strata of the central uplift (Fig. 12). Red Wing Creek is estimated to be 200 ± 25 Ma old, but the source of the hydrocarbons is Carboniferous Mississippian strata, i.e. 360–320 Ma old. It is a complex impact structure, ~ 9 km in diameter, with a central peak in which strata have been uplifted by up to 1 km (Brenan et al. 1975). When the central uplift was drilled in 1972, approximately 820 m of Mississippian oil column, with considerable high-angle structural complexity and brecciation and a net pay of approximately 490 m, was discovered. Beyond the structure, dips are gentle and the oil column is ~ 30 m. In this case, the hydrocarbon resources are progenetic but were physically displaced in the formation of the impact structure, resulting in enhanced accumulations and permeability of reservoir rocks in the central structural uplift. Primary and secondary recoverable reserves are estimated at 60–70 million barrels of oil and 100 billion cubic feet of gas (Donofrio 1998). Virtually all the oil has been discovered within a diameter of 3 km, corresponding to the central uplift. Based on net pay and its limited aerial extent, Red Wing is the most prolific oil field in the USA, in terms of producing wells per km^2, with the wells having the highest cumulative productivity of all wells in North Dakota.

Ames

The Ames structure in Oklahoma, USA, is a complex impact structure ~ 14 km in diameter. It is buried by up to 3 km of Ordovician to Recent sedimentary rocks and sediments (Carpenter and Carlson 1992). The structure was discovered in the course of oil exploration in the area and is the principal subject of a compilation of research papers in Johnson and Campbell (1997). The rim of the structure is defined by the structurally elevated Lower Ordovician Arbuckle dolomite. More than 600 m of Cambrian–Ordovician strata and some underlying basement rocks are missing in the centre of the structure due to impact. The entire structure is covered by the Middle Ordovician Oil Creek shale, which forms both the seal and source for hydrocarbons.

Initial oil and gas discoveries were made in 1990 from an approximately 500 m thick section of Lower Ordovician Arbuckle dolomite in the rim (Fig. 13). Wells drilled in the centre failed to encounter the Arbuckle dolomite and bottomed in granite breccias of the central uplift and, closer to the rim, in granite-dolomite breccias. These central wells produce over half the production from Ames and include the Gregory 1-20, which is the most productive oil well from a single pay zone in Oklahoma, flowing at the maximum regulated rate in Oklahoma and producing > 100,000 barrels of oil per year (Carpenter and Carlson 1992). Gregory 1-20 encountered an approximately 80 m section of granite breccias below the Oil Creek shale, with very effective porosity. A drill-stem test of the zone flowed at approximately 1300 barrels of oil per day, with a conservative estimate of primary recovery in excess of 5 million barrels from this single well. Conservative estimates of primary reserves at Ames suggest they exceed 25–50 million barrels of oil and 15–20 billion cubic feet of gas (Donofrio 1998). Hydrocarbon production is from the Arbuckle dolomite, the brecciated granite and granite-dolomite breccias and is largely due to impact-induced fracturing and brecciation, which has resulted in significant porosity and permeability. In the case of Ames, the impact not only produced the required reservoir rocks, but also the paleo-environment for the deposition of post-impact shales that provided the source of the oil and gas, upon subsequent burial and maturation. That is, the reservoir is syngenetic and the hydrocarbons are epigenetic.

There are similarities between the Ames crater shale and locally developed Ordovician shale in the Newporte structure in North Dakota, USA, an oil-producing (~ 120,000 barrels per year) 3.2 km diameter simple impact crater in Precambrian basement rocks of the Williston Basin. The Ames and Newporte discoveries have implications for oil and gas exploration in crystalline rock underlying hydrocarbon-bearing basins. Donofrio (1981) first proposed the existence of such hydrocarbon-bearing impact craters and that major oil and gas deposits could occur in brecciated basement rocks.

Campeche Bank

The Campeche Bank in the SE segment of the Gulf of Mexico is the most productive hydrocarbon-producing area in Mexico. The bulk of the hydrocarbons, from Jurassic source rocks (progenetic), are recovered from breccia deposits (syngenetic) at the Cretaceous–Paleogene (K–Pg) boundary. This area includes the world-class Cantarell oil field (Santiago-Acevedo 1980), which has produced over 11 billion barrels of oil and 3 trillion cubic feet of gas, between discovery in 1976 and 2006. Primary reserve estimates range as high as 30 billion barrels of oil and 15 trillion cubic feet of gas. Production is from up to 300 m of K–Pg dolomitized limestone breccias, with a porosity of around 10%. The seal rocks are a bentonitic bed, with shocked materials, and are altered ejecta materials from the K–Pg impact structure Chicxulub, which lies some 350–600 km to the NE. Grajales-Nishimura et al. (2000) proposed the following sequence of events for the K–Pg lithologies. What were to become the main, hydrocarbon-bearing breccias resulted from the collapse of the offshore carbonate platform due to seismic energy from the Chicxulub impact. This was followed by the deposition of K–Pg ejecta through atmospheric transport. Subsequent dolomitization of the ejecta and Tertiary tectonics served to form the seal and trap, respectively, for migrating Jurassic hydrocarbons. The net result was the creation of oil fields that account for > 60% of Mexico's hydrocarbon production and have reserves in excess of the entire onshore and offshore traditional hydrocarbon reserves of the USA, including Alaska (Donofrio 1998). The Cantarell oil field is now in decline, with production falling from a peak of around 2 million barrels per day in 2003 to 770,000 barrels per day in 2009, when it was superseded by the adjacent Ku-Mallop-Zaap field as the most productive oil field in Mexico. Oil from the Campeche Bank accounts for the bulk of the > US$35 billion of hydrocarbons (oil at $50 a barrel) produced from North American impact structures per year.

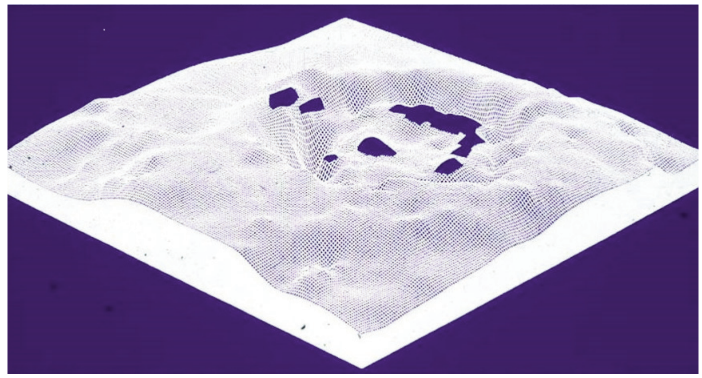

Figure 13. Three-dimensional mesh diagram of the topography on post-impact Slyvan shale at the complex Ames structure, USA. View is to NW at 25° elevation, with 20 times vertical exaggeration. Solid areas are hydrocarbon producing zones in the underlying Ames structure.

In summary, economic deposits associated with terrestrial impact structures range from world-class to relatively localized occurrences. There is increasing evidence that post-impact hydrothermal systems at large impact structures are of importance, with respect to their potential to redistribute metals. Such hydrothermal systems can blur the clear distinction between purely progenetic, syngenetic and epigenetic ore deposits related to impact. Although Vredefort and Sudbury are world-class mining districts, hydrocarbon production dominates the annual monetary value of natural resource deposits at impact structures. Commercial hydrocarbon accumulations are generally located in the central structural uplift of complex structures and in the rim areas of both complex and simple structures. While spatially localized, such accumulations occur

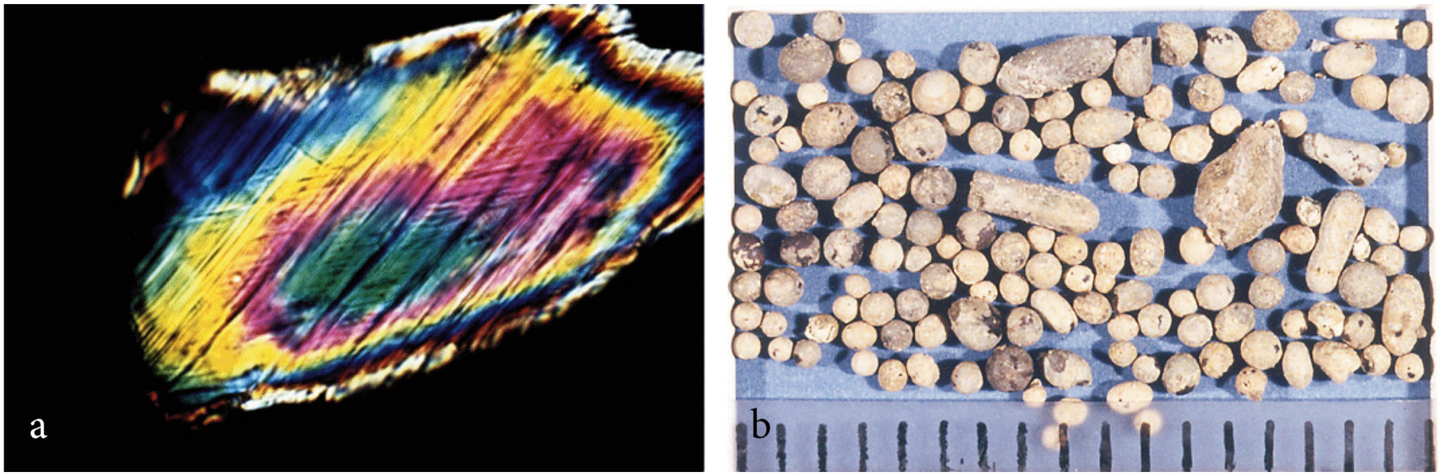

Figure 14. a) Shocked quartz displaying planar deformation features (PDFs) from the K–Pg boundary at Teapot Dome, USA. Length of grain is ~ 0.3 mm. Image from G. Izett, USGS. b) Impact spherules from the K–Pg boundary at Beloc, Haiti. Tick marks on scale are mm. Image from D.A. Kring, Lunar and Planetary Institute.

for a variety of reasons, including the physical redistribution of existing reservoir and seal rocks and brecciation to form reservoir rocks for migrating hydrocarbons. Many terrestrial impact structures remain to be discovered and, as targets for resource exploration, their relatively invariant morphological and structural properties, as a function of diameter, provide an aid to the development of efficient exploration strategies, particularly for hydrocarbons.

IMPACT AND THE PHANEROZOIC BIOSPHERE

The first suggestion that a large impact event may have resulted in the extinction of the dinosaurs at the end of the Cretaceous (K–Pg boundary) was by De Laubenfels (1956). No evidence, however, was presented beyond drawing analogies between the effects of the Tunguska atmospheric explosion in Siberia in 1908 and what would be the result of a much larger impact event. The first evidence that such an impact event had, in fact, occurred was the discovery of the geochemical signature, in the form of elevated PGE values, of meteoritic material in K–Pg boundary sedimentary rocks (e.g. Alvarez et al. 1980; Ganapathy 1980). This was followed by physical evidence through the identification of shocked quartz, with PDFs (Fig. 14; Bohor et al. 1984). The working hypothesis for the involvement of impact in defining the K–Pg boundary and as a cause of the associated mass extinction event was not without challenges (e.g. Officer et al. 1987). Much of the controversy was muted with the (re)discovery of the K–Pg impact site in the form of the buried Chicxulub impact structure in the Yucatan, Mexico (Fig. 15; Penfield and Camargo 1981; Hildebrand et al. 1991). Chicxulub itself was not without its debates, particularly centred on its size and form (e.g. Sharpton et al. 1996), which have largely been settled (~ 180 km in diameter, peak ring basin) through a series of offshore reflection seismic profiles (e.g. Morgan et al. 1997). The K–Pg boundary is now known from over 350 sites world-wide and a vast and diverse literature exists on its characteristics with respect to the Chicxulub impact. The most recent compilation and review of this literature making the case for a global correlation between Chicxulub, the impact evidence in K–Pg boundary deposits,

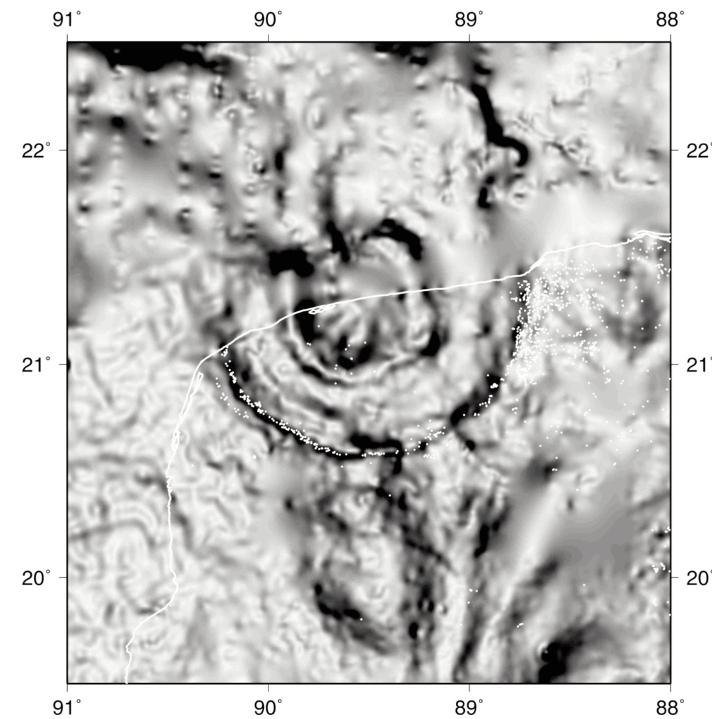

Figure 15. Greyscale image of horizontal gravity gradient over the buried K–Pg structure Chicxulub, Yucatan, Mexico. Solid white line defines the coast line with the Gulf of Mexico. Gravity image of the structure is better defined on-shore, due to spacing of gravity measurements. White dots are sink holes (cenotes). Groundwater flow is to the north and is deflected around the rim of the structure.

their variation in character with distance from Chicxulub (e.g. Fig. 14) and the attendant mass extinction event can be found in Schulte et al. (2010). It is not repeated here, in detail. Despite this weight of evidence, however, detractors of the impact working hypothesis remain (e.g. Keller et al. 2010).

The most outstanding questions centre on the details of the geology and structure of Chicxulub itself and on how this impact event led to severe global environmental degradation. With respect to the former, reflection seismic has clearly defined a topographic peak ring within the structure (e.g. Morgan et al. 2011). From the point of view of impact mechanics, the exact formational mechanism of peak rings is a topic of debate. Currently, there are two major working hypotheses; one based on numerical models (e.g. Collins et al. 2002, 2008; Ivanov 2005), and the other a conceptual geological model based on planetary (Mercury and moon) observations and interpretations (e.g. Head 2010; Baker et al. 2011a, b). The most recent review of the nature and constraints on peak ring formation, as provided through imagery and altimetry from the Lunar Reconnaissance Orbiter, in comparison with recent numerical models, is somewhat equivocal as to supporting, or not, differing working hypotheses for the formation of peak rings (Baker et al. 2016). Baker et al. (2016) note specifically that "Unfortunately, *in situ* samples of peak rings have not been obtained from the Moon to aid in distinguishing between the scenarios described".

Equally unfortunately, the terrestrial impact record is not particularly forthcoming when it comes to the subject of peak rings. Peak rings occur only in large impact basins of which there are limited examples preserved on Earth. A combination of observations, interpretations and logical arguments suggests that the three largest known impact structures on Earth: Vredefort, Sudbury and Chicxulub, all had some form of peak ring (Grieve et al. 2008). Only Chicxulub, however, has a preserved topographic peak ring. The exact character of the peak ring at Chicxulub is currently being investigated through a recently completed joint IODP-ICDP drilling expedition (Morgan et al. 2015). The initial analysis and interpretation of this core is compatible with the working hypothesis of the collapse of an over-heightened central peak as the mechanism for peak ring formation, which is a feature of the numerical models (Morgan et al. 2016).

It is hoped that the analysis of this core will also provide some constraints on the nature of the impact-induced 'killing mechanism' for the Cretaceous biosphere. The initial kinetic energy of the body that resulted in the formation of Chicxulub is estimated to have been ~ 5×10^{23} J. To put this in context, the energy released was ~ 5×10^{3} times greater than the annual output of internal energy of the entire Earth of ~ 10^{20} J. While this is an immense amount of energy, most of it was contained at the impact site in the formation of the impact structure and in the melting and vaporization of the target rocks. There is evidence of catastrophic 'local' effects (seismic and tsunami events) and the air blast and wildfires from the impact event would have been, at least, sub-continental in scale (Grieve and Kring 2007). These, however, would not have resulted in the evidence for environmental degradation on a global scale at the K–Pg boundary. To be global, the effects on the Chicxulub impact event have to be coupled through the atmosphere.

In this regard, the initial working hypothesis was that the impact event ejected sufficient sub-micrometre dust into the stratosphere so that photosynthesis effectively ceased and the global food chain collapsed (Alvarez et al. 1980). Initial modelling of such dust loading estimated > 10^{17} g of sub-micrometre dust from the Chicxulub event, compared with 10^{16} g required to result in the cessation of photosynthesis (Toon et al. 1997). The problem with this working hypothesis is that, by analogy with Chicxulub, smaller impact events, such as the Manicouagan event in Quebec (100 km diameter, 214 ± 1 Ma), would have produced 10^{16} g of stratospheric sub-micrometre dust but they did not result in a global mass extinction event (Grieve and Kring 2007). To compound difficulties with the initial working hypothesis, modelling of the Chicxulub event and its interaction with the atmosphere indicated that, although the impact-related fireball that reached above the Earth's atmosphere contained > 10^{18} g of material, most of this material was initially in the form of vapour and re-entered the Earth's atmosphere as condensation droplets in the hundreds of micrometres size range (e.g. Toon et al. 1997; Pierazzo et al. 1998). In addition, more recent analysis estimates that the total mass of clastic debris in the fireball and available for global distribution through the atmosphere is < 10^{16} g and of that < 10^{14} g is sub-micrometre in size (Pope 2002), i.e. well below the atmospheric dust loading required for the cessation of photosynthesis.

Soot has been discovered in the K–Pg boundary layer and the occurrence of global wildfires has been proposed as one of the major deleterious effects of the Chicxulub impact (e.g. Woolbach et al. 1990). The total mass of combusted carbon is estimated to be close to 10^{17} g, which is actually greater than expected from the global burning of all vegetation at the time of the K–Pg event (Woolbach et al. 1990). It has been suggested that in addition to setting vegetation alight, the impact event and what followed resulted in the combustion of all organic material at the impact site, as well as oil seeps, coal beds, etc. There are two major ignition sources in an impact event the size of Chicxulub: the impact fireball of hot melt and vapour and the heating of high-velocity, impact ejecta re-entering the Earth's atmosphere. The impact fireball, however, will only ignite fires close to the impact site. Scaling from much smaller events, such as Tunguska and nuclear weapon tests, have considerable uncertainty but place some limits on the ability of the fireball to ignite vegetation, with estimates ranging from radial distances from the impact site of ~ 1250 km (Toon et al. 1997) to as much as ~ 3000 km (Shuvalov and Artemieva 2002).

Only thermal radiation from re-entering ejecta has the potential to produce wildfires on a global scale at the K–Pg boundary. Initial models of the thermal pulse associated with the re-entry of ejecta have suggested thermal radiation of > 10 $kW.m^{-2}$ over some 20 minutes (e.g. Melosh et al. 1990), sufficient to ignite global wildfires. Subsequent, more complex models, acknowledged that not all the thermal radiation from re-entering ejecta reached the Earth's surface and that there was a component of self-shielding with respect to the radiation from later arriving ejecta, which could reduce the thermal pulse to 5 $kW.m^{-2}$ and only for several minutes. This would be sufficient to ignite tinder but not living vegetation (Goldin and Melosh 2009). It has been argued, however, that such a scenario would lead to the subsequent ignition of global wildfires (e.g. Robertson et al. 2013). It has also been noted that the global distribution of re-entering ejecta will not be uniform, as assumed in some model calculations, and will be affected by such parameters as the impact angle and direction, and the

https://doi.org/10.12789/geocanj.2017.44.113

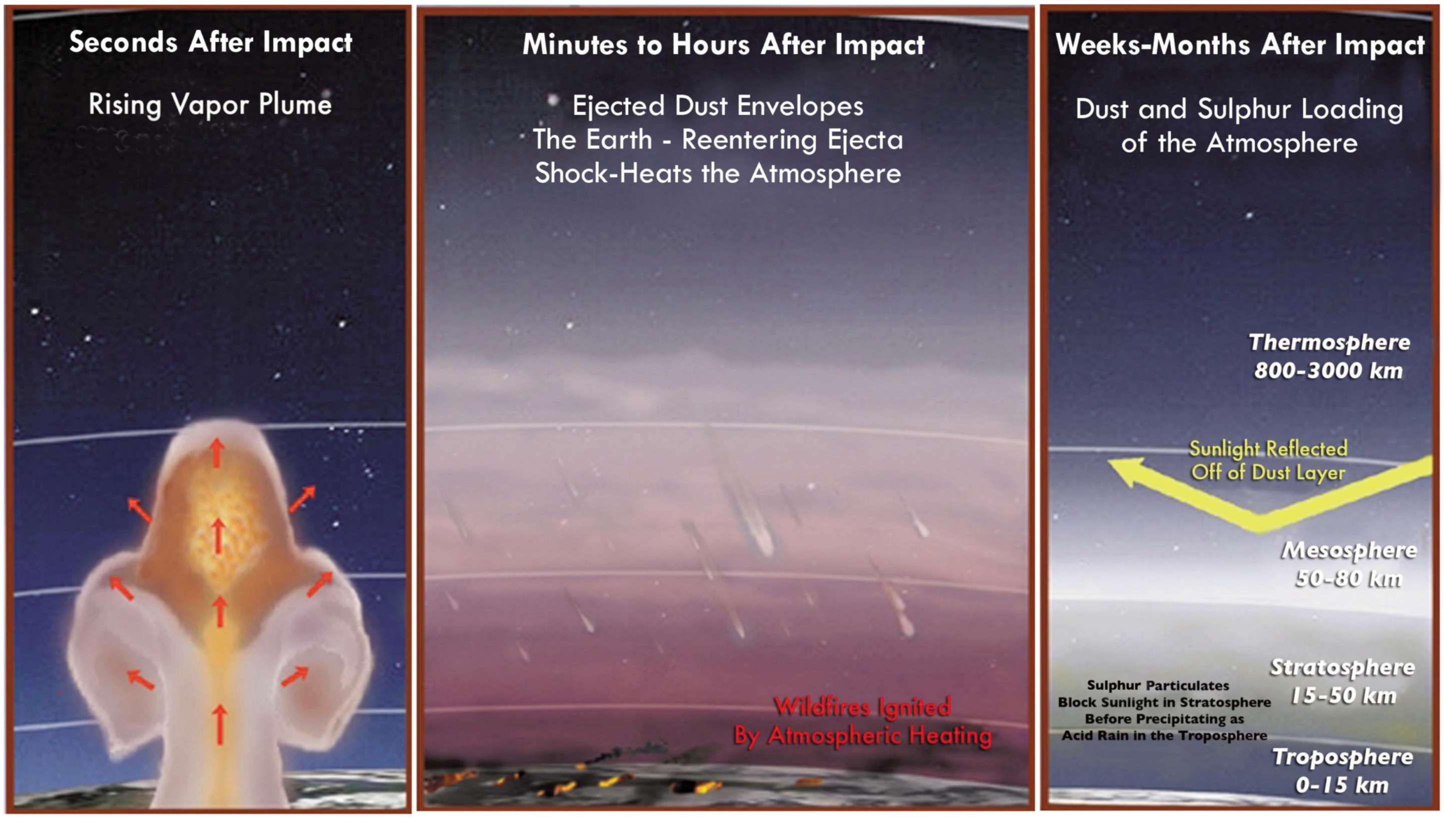

Figure 16. Scenario for the evolution of the degradational effects on the environment by the K–Pg impact event. Modified from an original diagram by D.A. Kring, Lunar and Planetary Institute.

Earth's rotation. Also, ejecta re-entry times will span a few days after the impact and will not be uniform over this time interval (e.g. Kring and Durda 2002). This more complex scenario is acknowledged in some recent modelling (e.g. Morgan et al. 2013), with the general conclusion that the thermal radiation from the Chicxulub impact will not be distributed uniformly over the Earth's surface and wildfires directly from the impact will not be global in extent. Nevertheless, the thermal pulse will lead to desiccation of vegetation and the effects of global cooling and darkness will cause widespread die off in vegetation and leave it extremely susceptible to fires ignited by such things as lightning strikes, i.e. the global soot at the K–Pg boundary may be the result of both impact-related and post-impact wildfires.

One feature of the Chicxulub impact site that may have been critical with respect to the impact resulting in a global mass extinction event is that it contained anhydrite in the target rocks. Although estimates vary by orders of magnitude, the amount of sulphur released by the impact was ~ 10^{16}–10^{18} g (e.g. Pope et al. 1997; Kring 2007). While the small portion of the sulphur aerosols contained in the atmosphere would have likely combined with water vapour to produce acid rain, this would not have been sufficient to acidify the oceans, although it may have had more local effects in shallow environments and continental watersheds. Sulphur aerosols are much more efficient in reducing solar radiation reaching the Earth's surface than dust and are the main cause of such reductions and cooling due to volcanic eruptions. For example, some 10^{13} g of sulphur was released into the lower stratosphere during the 1991 Mt. Pinatubo eruption, resulting in a cooling of the surface of ~ 0.5°C for several years (Ward 2009). By comparison, the K–Pg impact is considered to have produced 3–5 orders of magnitude more sulphur aerosols. A number of other chemically active gases and deleterious atmospheric changes (e.g. oxides of nitrogen due to shock and later ejecta re-entry heating of the atmosphere) would have been produced by the K–Pg impact event (e.g. Kring 2004).

At this time, there is no definitive, single causative impact-related agent for the K–Pg mass extinction event and it may have been a combination of effects (dust and sulphur aerosol loadings, massive wildfires, atmospheric changes and global cooling (Fig. 16; Pope et al. 1994, 1997)). As noted, it is hoped that the results of the recently completed joint IODP-ICDP drilling project within Chicxulub will provide further resolution and constraints (e.g. Morgan et al. 2015; 2016). Based on modelling and logical inference of the results of the Chicxulub impact, the post-K–Pg impact world, however, must have been a 'hellish' place of cold, darkness, choking fumes and acid rain; all leading to the global collapse of both the marine and terrestrial food webs. Analogies have been made with the results of a catastrophic 'nuclear winter' (e.g. Toon et al. 1997). Until recently, unequivocal evidence for the working hypothesis of a K–Pg 'impact winter' has been lacking, due largely to the absence of climatic records of sufficient temporal resolution. The recent results of high resolution organic TEX_{86} paleothermometry on three cores spanning the K–Pg boundary in

New Jersey, USA, however, indicate a sharp drop in temperature of ~ 3°C, coinciding exactly with the K–Pg boundary (Vellekoop et al. 2016).

Although there have been controversial claims of other impact-related extinctions in the terrestrial record (e.g. the temporal relation between the so-called Bedout High and the Permian–Triassic mass extinction event (Becker et al. 2001, 2004)), no evidence such as that from Chicxulub and the K–Pg boundary sedimentary rocks has been forthcoming. Impact events on the scale of Chicxulub, however, are estimated to occur on Earth on time-scales of ~ 100 Ma (Toon et al. 1997). Given that impact is a process governed by physics, impacts of similar scale on a given planetary body will produce similar results. The one variable that has the potential to modify this is changes in the type of target material. This has only minor effects on the cratering process *per se* but may well be significant with respect to the effects of the impact on changes to the atmosphere. Given that Chicxulub appears unique with respect to its effect on the Phanerozoic biosphere, it suggests that sulphate-bearing lithologies in the Chicxulub target may be the significant variable with respect to the effects of this particular large-scale impact on the terrestrial atmosphere and, thus, biosphere.

It has been suggested that impacts smaller than Chicxulub will produce severe effects to the 'local' biosphere and may be responsible for some of the sudden, short-term climatic disruptions, as mirrored by stable isotope excursions in the stratigraphic record (Grieve 1997). For example, a 25 mm thick ejecta layer dated at 214 ± 2.5 Ma and believed to be from Manicouagan (214 ± 1 Ma) has been reported from near Bristol, UK (Walkden et al. 2002). The surface blast wave from an event such as Manicouagan would have wind speeds of over 1000 $km.s^{-1}$ near the impact site and be sufficient to kill and injure exposed plant and animal life out to a radius of ~ 550 km (Grieve and Kring 2007). A late Eocene carbon and oxygen isotope anomaly has been ascribed to the almost simultaneous impacts that formed the Chesapeake Bay (40 km diameter, 35.5 ± 0.3 Ma) and Popigai (100 km diameter, 35.7 ± 0.2 Ma) impact structures (Vonhof et al. 2000). A ^{12}C anomaly and, most recently, what are interpreted to be impact-related spherules (Fig. 17) and shocked quartz have been discovered at the Paleocene–Eocene boundary and a case made for an impact trigger for the Paleocene–Eocene Thermal Maximum (PETM) 56 Ma ago (Kent et al. 2003; Schaller et al. 2016).

IMPACT AND THE EARLY EARTH

Precambrian

Although many terrestrial impact structures occur on Precambrian Shield and cratonic areas of the crust, due to their intrinsically low erosion rates and greater deformational stability, the record of Precambrian-aged structures is relatively sparse. This is due to their formational-age and is reflected in the previously noted fact that the known terrestrial impact structures are a preservation sample of an originally more numerous population. The Precambrian record does include two of the largest known structures; Sudbury and Vredefort (Vredefort being the oldest and largest with an age of ~ 2.02 Ga and an estimated original diameter of ~ 300 km). The dominant record of impact in the Precambrian is in the form of spherule beds, which are considered to have an impact origin, in supracrustal successions between ~ 3.47 and ~ 2.49 Ga in age (Lowe et al. 2014). These beds occur in South Africa and Australia and range from ~ 1 cm to a few 10's of metres in thickness. Various lines of evidence have been presented to support an impact origin, including near chondritic platinum group element ratios, extra-terrestrial chromium isotopic compositions and the presence of nickel-rich chromite (e.g. Kyte et al. 2003; Simonson et al. 2009; Lowe et al. 2014). At least 18 such spherule beds are known, with the latest discovery being an ~ 3.46 Ga example in Western Australia (Glickson et al. 2016).

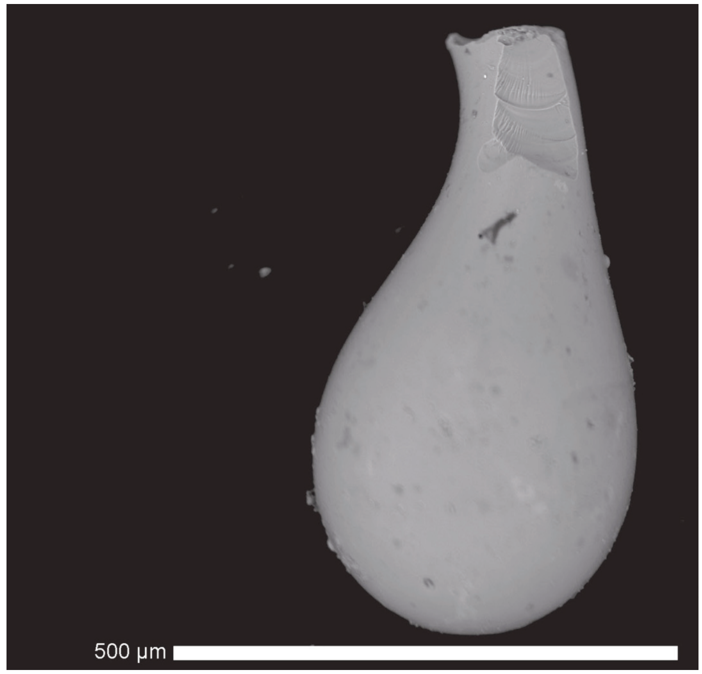

Figure 17. Impact spherule from the Paleocene–Eocene–Thermal Maximum in Milliville drill hole (ODP, Leg 174AX). Image from M. Schaller, Rensselaer Polytechnical Institute.

Impact-related spherule beds are known from the Phanerozoic, e.g. tektites and micro-tektites (e.g. Simonson and Glass 2004) and from the preserved ejecta of such impact structures as Chicxulub and Sudbury (e.g. Addison et al. 2005). These spherules, however, are generally accompanied by evidence of sub-solidus shock effects, such as quartz with planar deformation features. In the case of these Precambrian spherule beds, there has been only one case of reported sub-solidus shock in the form of a single shocked quartz grain (Rasmussen and Koeberl 2004). The apparent dearth of sub-solidus shocked material could be attributed to the age of these beds, with such features as planar deformation features having completely annealed out over time. Most recently, however, the high pressure polymorph TiO_2-II, which is known to occur in impact deposits (e.g. Jackson et al. 2006), has been reported from four Neoarchean spherule beds (Smith et al. 2016).

Questions, however, remain. In particular, why are there so many apparently impact-related spherule beds over a relatively limited time period, compared to the remainder of the terrestrial sedimentary record? This could be simply an aberration with respect to preservation of the record. Also, it is generally assumed that such beds are the product of large impact events (e.g. Glickson et al. 2016), with analogies with Chicxulub and its ejecta the most common. The lunar impact record suggests that the impact-rate in the Earth-moon system at this time was not much higher than in the Phanerozoic (Fig. 18; Stöffler et al. 2006). A minimum of 18 such events, however, in an ~ 1 Ga time-period suggests that possibly impacts smaller than Chicxulub could produce such spherule beds.

Hadean

It is generally believed that the terrestrial planets formed in a similar manner through the rapid accretion of planetismals and planetary embryos over a relatively short period of a few tens of millions of years (e.g. Chambers 2004). This rapid accretion and the conversion of accretional kinetic energy into heat resulted in the formation of magma oceans, leading to the primary differentiation of the terrestrial planets and the formation of their initial crusts. From then, further evolution of the terrestrial planets diverged, depending on their size (thermal regime, planetary gravity) and the presence or absence of water. Another commonality is that, following the formation of their initial crusts, they continued to be subjected to an intense impact regime over the time period of what is referred to as the Hadean (~ 4.5–3.9 Ga), in the case of the Earth. The evidence for such an early period of intense bombardment is most compelling on the smaller and less evolved terrestrial planets, such as the moon and Mercury, in the form of a multitude of impact craters, including multiring basins, some with diameters in excess of 1000 km. Reasoned speculation and theoretical modelling considerations on the effects of this bombardment on the Hadean Earth have included the sterilization of the Earth's surface and its role in delivering and inhibiting the development and evolution of life (e.g. Thomas et al. 1997), the erosion of the primordial atmosphere (e.g. Melosh and Vickery 1989) and the boiling-off of portions, if not all, of the primordial hydrosphere (e.g. Zahnle and Sleep 1997).

In terms of the effects of such an early bombardment on terrestrial crustal evolution, many works explicitly acknowledge that such a bombardment took place but largely ignore any effects on crustal evolution (e.g. Harrison 2009). Early models of the effects of such a bombardment on the early Earth relied heavily on analogies with what is inferred with respect to the effects of such a bombardment on lunar crustal evolution, with allowances for a different thermal regime, higher planetary gravity and the presence of water (e.g. Green 1972; Frey 1980; Grieve 1980). At the time, however, a fundamental property of impact processes, which has been termed "differential scaling" (Grieve and Cintala 1992), was not recognized. As a result of this property, strict analogies between lunar and terrestrial impacts of similar size, particularly, with respect to the volumes of impact melt generated are not valid and very large lunar impacts, such as those that produced the multiring basins, are poor analogies for similar-sized impacts on the Hadean Earth.

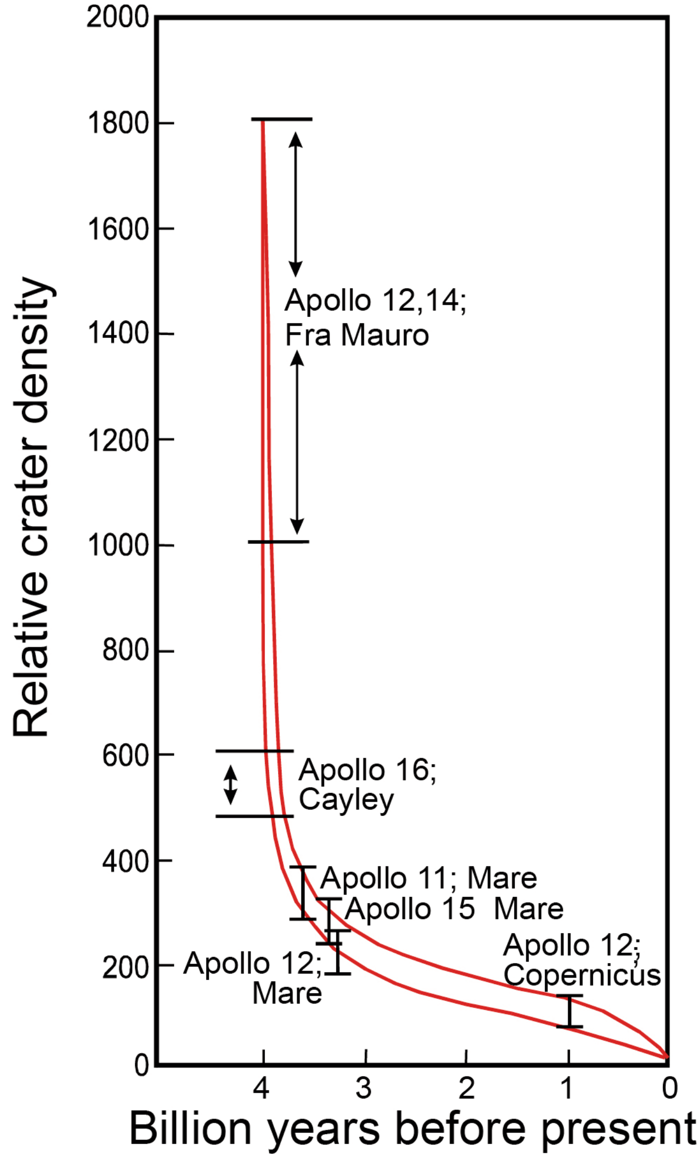

Figure 18. Variation in relative crater density for craters > 4 km diameter on the moon, with age of counting surface. Envelope of curves can be taken as a proxy for the variation in the cratering rate with time in the Earth-moon system. Note the steep rise in the cratering rate for ages > 3.8 Ga. The rate for ages < 3.5 Ga is essentially constant.

Differential scaling refers to the fact that planetary gravity is a primary variable in determining the efficiency of a given impact to form a crater of a given size. As it is a force that inhibits crater growth and includes a time term, cratering efficiency is reduced on higher gravity planetary bodies and in larger, compared to smaller, impacts. Thus, the effects of gravity are most pronounced in comparing large impact structures between bodies such as the Earth and moon. Gravity, however, is not a primary variable in the magnitude and geometry of the shock wave in the target and, thus, the volume of impact melt produced in a given impact, although planetary gravity affects impact velocity, with higher velocities resulting in more melt. In the case of the Earth, the volume of impact melt produced in an impact that would result in a several hundred kilometre

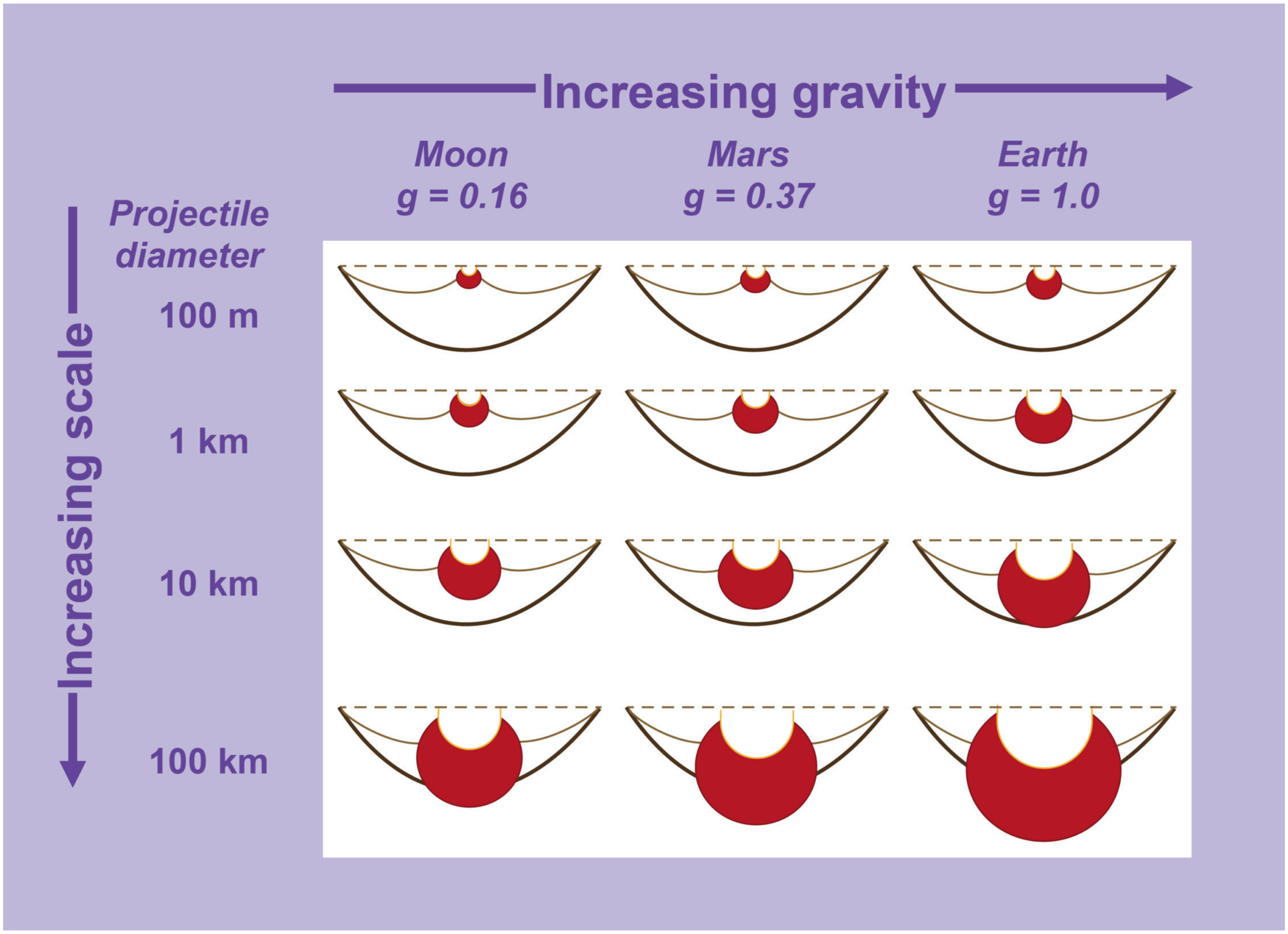

Figure 19. Schematic cross-section representation, scaled to transient cavity size, of the concept of differential scaling. Indicated are melt (red), transient cavity (solid) and ejected (dashed) areas, with increasing gravity (g), relative to the Earth (left to right) and increasing event size (top to bottom), all other impact parameters being fixed for the respective planetary bodies.

diameter crater on the moon exceeds that of the volume of the transient cavity produced by the cratering-flow field (Fig. 19). Thus, in terms of large impact events occurring on the Hadean Earth, the net result would not be final craterforms resembling their lunar counterparts produced by equivalent magnitude impacts. As melt has no strength, the resultant craterform would be extremely shallow, at best, and, most likely, conform more to a massive melt pool than recognizable craterforms.

The depths of these melt pools would have been variable and in the range of many kilometres to many tens of kilometres. What seems clear is that the surface and crust of the Hadean Earth would have had extensive and voluminous impact-produced melt pools of mafic composition, assuming an initial basaltic crust (Fig. 20). Given the appropriate cooling times, bodies of basaltic melt > 300 m thick differentiate in the terrestrial environment, with the potential degree of differentiation being a function of the thickness of the melt body (Jaupart and Tait 1995). It is, therefore, expected that these thick, closed-system melt pools would have differentiated into an ultramafic-mafic base and a more felsic top, much in the same manner as the ~ 2.5 km thick impact melt sheet, now manifested as the Sudbury Igneous Complex, at the originally ~ 150–200 km diameter Sudbury impact structure, Canada (Therriault et al. 2002). The results of individual impacts on the Hadean Earth would have been impressive. For example, a terrestrial impact event with the magnitude of the one that resulted in the Orientale basin on the moon would have generated in excess of 10^7 km^3 of impact melt. If only 10% of the initial melt volume took the form of felsic differentiates, they would have been comparable in volume to the Columbia River basalts.

The impact rate in the Hadean can be estimated from the lunar record of impacts for the same time period (Fig. 18). As the Earth has a larger gravitational cross-section than the moon, the impact rate will have been higher. How much higher, depends on the approach velocity of the impacting bodies, with slower approach velocities, which are generally considered

https://doi.org/10.12789/geocanj.2017.44.113

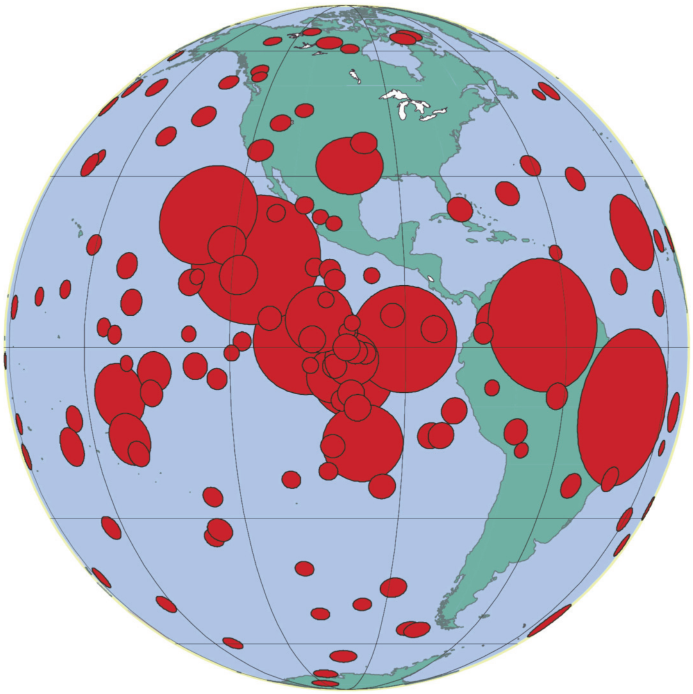

Figure 20. Cartoon of the number of impact melt pools (approximated by transient cavity diameters), where melt volumes exceed transient cavity volumes on the Hadean Earth. This is a minimum number, as the impact velocity was constrained to 22.4 km.s^{-1} (Table 2), close to the present-day average asteroidal impact velocity. Number of melt pools was estimated based on the lunar cratering record, scaled to terrestrial conditions (Grieve et al. 2006). Locations of melt pools were based on random numbers and current land masses are shown for scale.

to be the case in early solar system history, increasing the gravitational cross-section ratio (Table 2). With the lunar record as a proxy, such cumulative effects as the total amount of impact melting (as high as ~ 10^{12} km^3) can be estimated (Table 2). Such a range of cumulative effects can be found in Grieve et al. (2006). In essence, it suggests a Hadean Earth with a surface dominated by melt-pools, some of which were sub-continental in scale. Most recently more sophisticated modelling, using Monte Carlo simulations (5000 times) to calculate the impact flux and hydrocode simulations to calculate impact melting, reached similar conclusions (Marchi et al. 2014).

There are few rocks older than 4.0 Ga and the lithological nature of the Hadean depends on the interpretation of Hadean detrital zircons. The Ti-in-zircon crystallization temperature of these zircons is relatively low (~ 685°C) and felsic mineral inclusions have suggested crystallization from anatectic granitic melts (e.g. Cavoise et al. 2004; Watson and Harrison 2005) and by implication some form of plate tectonic processes operating in the Hadean (e.g. Hopkins et al. 2008). Grieve et al. (2006) suggested that, by analogy with the Sudbury Igneous Complex, such zircons could have also been produced in the more felsic components of differentiated impact melt sheets. Direct tests on zircons from the Sudbury Igneous Complex appeared to contradict this, in terms of crystallization temperatures for its zircons that were too high (Wielicki et al. 2012). Most recently, however, measurements on a more complete suite of samples from the Sudbury Igneous Complex, and using ion microprobe analyses, have indicated zircon crystallization temperatures overlapping that of Hadean zircons (Kenney et al. 2016). These results serve to revive the hypothesis that Hadean zircons could result from differentiated impact melt sheets, although they do not preclude an origin by more conventional plate tectonic-like processes. In their simulation of the impact history of the Hadean Earth, Marchi et al. (2014) argue that the peak in known Hadean zircon ages at 4.2–4.1 Ga coincides with the time, and is the result of, the so-called "Late Heavy Bombardment" in the Earth-moon system.

The most important impact in a planet's evolutionary history is the largest. The origin of the Earth's moon by such working hypotheses as capture, co-accretion and fusion all have severe difficulties, based on the size and composition of the moon and the angular momentum of the Earth-moon system (e.g. Hartmann et al. 1986). First suggested by Hartmann and Davis (1975), an alternate working hypothesis is that the moon is the result of the impact of a Mars-sized object, now named Theia (mother of the Greek moon goddess Selene) with the proto-Earth after core formation. This giant impact hypothesis was attractive in that it accounted for the unusual nature of the Earth-moon system compared to other planets and their satellites and was consistent with the origin of the moon not by an evolutionary but rather by a stochastic process in planetary dynamics. In computer simulations, a relatively low velocity oblique impact resulted in the formation of an iron-depleted accretionary disc around the proto-Earth from which an iron-poor moon formed and culminated in an Earth-moon system with the appropriate angular momentum (e.g. Canup and Asphaug 2001).

In these simulations, the material in the accretionary disc was largely from Theia's mantle. One of the main results of the analyses of lunar materials, however, is a remarkable simi-

Table 2. Relative asteroidal impact velocities and corresponding gravitational cross-sections for lunar and terrestrial impacts and culumulative impact melt produced on the Hadean Earth, in which melt volumes exceed transient cavity volumes (see text for details).

Impact velocity, moon, km.s^{-1}	Impact velocity, Earth, km.s^{-1}	Gravitational cross-section, moon, km^2	Gravitational cross-section, Earth, km^2	Ratio cross-section areas, Earth/moon	Cumulative impact melt volume, km^3
7.5	14.9	1.34×10^7	1.29×10^9	96.14	1.31×10^{12}
10	17.4	1.09×10^7	5.41×10^8	49.76	3.25×10^{11}
15	22.4	9.91×10^6	2.54×10^6	25.76	7.87×10^{10}

larity in composition with the Earth, particularly with respect to some isotopic ratios (e.g. Wiechert et al. 2001; Zhang et al. 2012). This requires that Theia's mantle was similar in composition to that of the Earth and, thus, Theia originated from a position in the solar system similar to that of the Earth. This is an unlikely scenario, given simulations of the formation of the terrestrial planets (e.g. Chambers 2001). More recent computer simulations, however, of the moon's origin by impact appear to have addressed the compositional similarity through high speed impact into a fast spinning proto-Earth or impacts with similar-sized bodies in that the resultant accretionary disc, from which the moon formed, is largely Earth mantle materials (e.g. Ćuk and Stewart 2012; Canup 2012).

Recent work on Pb isotopes suggests a major loss of volatile Pb relative to refractory U at 4.43–4.42 Ga on Earth and provides an age constraint on the timing of the moon-forming event by Connelly and Bizzarro (2016). They estimate a loss of ~ 98% of terrestrial Pb relative to solar system bulk composition by the moon-forming impact due to volatility. If Pb was lost during the moon-forming event, then more volatile materials, such as water, were also lost. This is in keeping with models that indicate the present inventory of terrestrial volatiles is from post moon-forming accreting chondritic materials (e.g. Albarede et al. 2013).

The moon (and its postulated effects) is a prominent feature of human culture and lore. Without a moon-forming impact event, however, the major effect of the lack of such a massive satellite on the Earth would have been the lack of lunar tides. With only solar tides, the extent of tidal zones to the world's oceans and seas would be reduced by ~ 55%. As such tidal zones represent the transition between the marine and terrestrial environments and biospheres, it can be speculated that such a reduction in their extent could well have affected the path and speed of terrestrial biosphere evolution.

IMPACTS AND THE FUTURE EARTH

The future impact of a sizeable extraterrestrial body on the Earth is inevitable. Relatively small events, such as the one that resulted in the famous ~ 1.2 km diameter Barringer or Meteor crater in Arizona, USA, some 50,000 years ago, and even those involving objects too small or weak to reach the ground, such as the 1908 Tunguska event in Siberia, Russia, have the capacity to have severe social and economic consequences, depending on the location of the event (e.g. Dore 2007). The most recent event was the February, 2013, air blast from the passage of an ~ 20 metre object at ~ 30–50 km altitude over the city of Chelyabinsk in the Urals, Russia (e.g. Brown et al. 2013). The shock wave damaged buildings and resulted in injuries to over 7,000 people, although there were no reported fatalities. Toon et al. (1997) found that impact events occurring on frequencies less than ~ 50,000 years produce blast damage, earthquakes, and fires over areas (10^4–10^5 km^2) that are similar in size to those affected by recent disasters. Readers wishing to know the potential effects at a specified distance of a specified impact event are referred to http://impact.ese.ic.ac.uk/ImpactEffects/. An ICSU-sponsored series of works dealing with the impact hazard and its effects (social, economic, potential deaths, etc.) can be found in Bobrowsky and Rickman (2007).

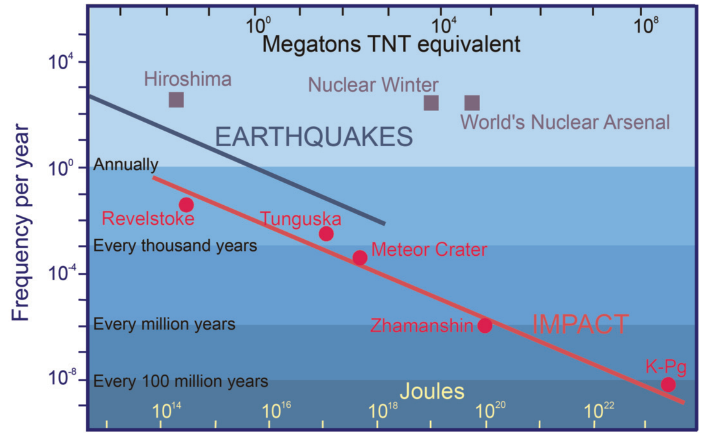

Figure 21. Logarithmic plot of frequency versus energy (J and TNT equivalent) of terrestrial impact events compared to earthquakes. Earthquakes are more frequent than impacts but have an upper limit to the energies involved. The energies and frequencies of some specific terrestrial impact events are indicated, as are the nuclear energies of the Hiroshima atomic bomb and those believed to be sufficient to result in a 'nuclear winter' and contained in the world's nuclear arsenal.

The threshold for disrupting human civilization is much less than that needed for a significant extinction event, such as at the K–Pg boundary. To affect global society, impacts have to be energetic enough to produce dust-loadings and other chemical changes in the atmosphere that result in short-term climatic changes, particularly cooling (MacCracken 2007). Since 75% of the Earth's surface is covered by water, impact-induced tsunamis may be a greater potential threat (e.g. Hills et al. 1994; Chapman 2004). The magnitude, however, of such a threat is somewhat controversial and uncertain, as it is most likely that the envisioned massive waves would collapse under their own weight, resulting in turbulence and the dissipation of the bulk of their energy relatively close to the impact point (e.g. Melosh 2007). Global consequences, however, of impacts into water may occur on time-scales of 300,000 years, when the impacts distribute water vapour and destroy ozone in the atmosphere (Birks et al. 2007), with larger impact events creating disasters beyond anything recorded in human history. Other natural disasters (e.g. hurricanes, earthquakes) occur more frequently than impact events (Chapman 2004). Impact events, however, can release vast amounts of energy (Fig. 21) and have the capacity of creating disasters of far greater magnitude than any other natural process. They are low probability but high consequence events, which can affect much larger regions, produce several environmental perturbations simultaneously and have essentially no upper limit to their energy release and, thus, severity.

SUMMARY REMARKS

Perhaps due to the wide range of highly active endogenic geologic processes on the Earth, the earth sciences were slow to recognize the evidence for the occurrence of impact events on Earth. The first terrestrial impact site (Barringer) was documented ~ 100 years ago, but its impact origin at the time was highly controversial. Focused exploration efforts on terrestrial

https://doi.org/10.12789/geocanj.2017.44.113

impact structures as geologic features, and lunar analogues, did not occur until the immediate pre-Apollo era. Today, the basic physical and chemical characteristics of terrestrial impact structures and how they vary in form with diameter have been documented. The characteristics clearly delineate them from other terrestrial geologic structures. Nevertheless, the number of known impact structures and records of impact in the stratigraphic record is small (~ 200) and it would be premature to state that the current sample is complete or that impact processes have truly entered into the mainstream knowledge base of the earth science community.

At present, some sixteen impact structures are known with diameters > 20 km and ages less than 100 Ma on the Earth's land surface. These had impact energies in excess of ~ 10^6 MT TNT equivalent (~ 4×10^{21} J) and were dramatic events that had potentially catastrophic regional environmental effects and moderate to severe continental and global effects. To put the potential of impact to affect catastrophic change in a more realistic perspective, the average impact cratering rate during the last 100 Ma is estimated to be $5.6 \pm 2.8 \times 10^{-15}$ $km^{-2}.a^{-1}$ for events that produce > 20 km diameter craters (Grieve 1984). This translates to ~ 85 impact events of such magnitude that actually occurred on the Earth's land surface in the last 100 Ma, i.e. the known sample is ~ 20% of the actual number of events that occurred. The largest, the end-Cretaceous Chicxulub impact, extinguished ~ 75% of species living at the time. This mass extinction provided evolutionary opportunities and surviving members of the extinction underwent massive adaptive radiations into the emptied ecological niches. Such ushered in the rise of mammals, which ultimately led to the evolution of humans. Chicxulub, and other impacts, have begun to demonstrate the regional to global environmental effects of impacts and evaluating their environmental and biologic effects is a critical step in the assessment of the hazards from future impact events Although such large impact events are regionally and/or globally important, smaller impact events can not be ignored on an Earth that has an ever-increasing population. Even Barringer-sized events have the potential to destroy a modern city. It is estimated that 1 km diameter cratering events occur every few thousand years (Neukum and Ivanov 1994). Impact airbursts, like Tunguska, which are also capable of considerable destruction, occur more frequently, perhaps every few hundred years. It is inevitable that human civilization, if it survives itself long enough, will be exposed to an impact-induced environmental crisis of potentially extreme proportions.

As the Chicxulub event and the subsequent biological evolutionary trends favouring mammals indicate, impact events are not entirely a negative phenomenon with respect to the current human condition. In addition, they represent unusual geological events and, as such, they have resulted in local anomalous geological environments, some of which have produced significant economic deposits. About 20% of known terrestrial impact structures have some form of economic deposit associated with them, and about half of these are currently exploited or have been exploited in the recent past. The deposits range from local and uneconomic (e.g. reserves of 3×10^5 t of hydrothermal Pb–Zn ores at Siljan, Sweden) to world-class (e.g. 1.5×10^9 t Ni–Cu–PGE ores at Sudbury) and also include significant (and sometimes unusual) hydrocarbon deposits.

With respect to crustal evolution, all the terrestrial planets were subject to a period of intense bombardment following their formation. What the result of this bombardment was for the Hadean can only be the subject of reasoned speculation. The argument advanced, here, is that such a period of bombardment would not result in the 100's–1000's km diameter multiring basins, as observed on the moon, but rather in immense pools of impact melt, due to the effect of the high planetary gravity on Earth and its effect in the phenomenon termed 'differential scaling.' Such silicate melt bodies, whether produced by igneous or impact processes, have the potential to differentiate. This is observed at the largest currently known impact melt sheet on Earth, the Sudbury Igneous Complex. The only known surviving products of the early Earth are Hadean-age detrital zircons in younger lithologies. Recent analyses indicate that the crystallization temperatures of zircons from the Sudbury Igneous Complex span the range of those in these Hadean zircons, effectively removing an objection to the hypothesis that Hadean zircons could be impact melt products. This reopens the door to the hypothesis that impact melt formation and differentiation was a mechanism to produce the earliest felsic lithologies of the Earth's crust. It does not, however, preclude other processes but suggests that the potential effects of this intense bombardment on early Earth's history can not be simply ignored.

Amongst the terrestrial planets, the Earth's moon is unique, particularly in terms of its size relative to the Earth. Although it may have a counterpart in the size relation between Pluto and its satellite Charon, this suggests a non-evolutionary, stochastic process may have been involved in its origin. The giant impact hypothesis on the proto-Earth at > 4.4 Ga is currently the favoured working model. Recent computer simulations indicate that it is possible to account for the isotopic similarities between the Earth and the moon, which was a major stumbling block in accepting some of the earlier modelling of such a moon-forming impact. Although sometimes forgotten in today's computational environment, however, the 'fact' that some phenomenon can be modelled and apparently satisfy the known evidence does not elevate the model, itself, to empirical evidence for that process. Nevertheless, it does appear to be a more satisfying working hypothesis than those previously advanced to account for the origin of the moon.

Although not detailed here, but with moon-forming impact as a context, it can be argued that impact is the most fundamental of the physical processes in Earth's history, as it was the process whereby the terrestrial planets, themselves, were formed and, in the case of the Earth, received its volatile budget. Finally, it can also be argued that the formation of the moon, the K–Pg mass extinction and the creation of exploitable natural resources by large-scale impact on Earth have all been positives towards the current evolution of humanity. Ultimately, however, the impact hazard must also be recognized as a reality and as a negative in the long-term extended future of humanity.

ACKNOWLEDGEMENTS

Much of my efforts to understand impact processes and their effects were undertaken in collaboration and in co-authorship with international colleagues, to whom I will always be grateful. In particular, I would like to acknowledge J. Garvin and M. Cintala (NASA), J. Head (Brown U.), J. Morgan (Imperial College), U. Riller (U. Hamburg), D. Stöffler (Humboldt U.), V. Masaitis (Karpinsky Institute), G. Osinski (Western U.) and A. Therriault and B. Robertson (GSC) for their stimulating intellectual interactions over the years. Thanks also go to M. Grieve for his efforts in providing the graphics and to A. Therriault for critical reading of this contribution. Formal reviews by F. Hörz and an anonymous reviewer are greatly appreciated.

REFERENCES

Abramov, O., and Kring, D.A., 2004, Numerical modeling of an impact-induced hydrothermal system at the Sudbury crater: Journal of Geophysical Research, v. 109, E10007, https://doi.org/10.1029/2003JE02213.

Addison, W.D., Brumpton, G.R., Vallini, D.A., McNaughton, N.J., Davis, D.W., Kissin, S.A., Fralick, P.W., and Hammond, A.L., 2005, Discovery of distal ejecta from the 1850 Ma Sudbury impact event: Geology, v. 33, p. 193–196, https://doi.org/10.1130/G21048.1.

Albarede, F., Ballhaus, C., Blichert-Toft, J., Lee, C-T., Marty, B., Moynier, F., and Qing-Zhu, Y., 2013, Asteroidal impacts and the origin of terrestrial and lunar volatiles: Icarus, v. 222, p. 44–52, https://doi.org/10.1016/j.icarus.2012.10.026.

Alvarez, L.W., Alvarez, W., Asaro, F., and Michel, H.V., 1980, Extraterrestrial cause for the Cretaceous–Tertiary extinction: Science, v. 208, p. 1095–1108, https://doi.org/10.1126/science.208.4448.1095.

Ames, D.E., and Farrow, C.E.G., 2007, Metallogeny of the Sudbury mining camp, *in* Goodfellow, W.D., *ed.*, Mineral Deposits of Canada: Mineral Deposits Division, Special Publication 5, Geological Association of Canada, St. John's, NL, p. 329–350.

Ames, D.E., Jonasson, I.R., Gibson, H.L., and Pope, K.O., 2006, Impact-generated hydrothermal system — Constraints from the large Paleoproterozoic Sudbury crater, Canada, *in* Cockell, C., Koeberl, C., and Gilmour, I., *eds.*, Biological Processes Associated with Impact Events: Springer-Verlag, Berlin, p. 55–100, https://doi.org/10.1007/3-540-25736-5_4.

Ames, D.E., Davidson, A., and Wodicka, N., 2008, Geology of the giant Sudbury polymetallic mining camp, Ontario, Canada: Economic Geology, v. 103, p. 1057–1077, https://doi.org/10.2113/gsecongeo.103.5.1057.

Baker, D.M.H., Head, J.W., Schon, S.C., Ernst, C.M., Prockter, L.M., Murchie, S.L., Denevi, B.W., Solomon, S.C., and Strom, R.G., 2011a, The transition from complex crater to peak-ring basin on Mercury: New observation from MESSENGER flyby data and constraints on basin-formation models: Planetary and Space Science, v. 59, p. 1932–1948, https://doi.org/10.1016/j.pss.2011.05.010.

Baker, D.M.H., Head, J.W., Fasset, C.I., Kadish, S.J., Smith, D.E., Zuber, M.T., and Neumann, G.A., 2011b, The transition from complex crater to peak-ring basin on the Moon: New observations from Lunar Orbiter Laser Altimeter (LOLA) instrument: Icarus, v. 214, p. 377–393, https://doi.org/10.1016/j.icarus.2011.05.030.

Baker, D.M.H., Head, J.W., Collins, G.S., and Potter, R.W.K., 2016, The formation of peak-ring basins: Working hypotheses and path forward in using observations to constrain models of impact-basin formation: Icarus, v. 273, p. 146–163, https://doi.org/10.1016/j.icarus.2015.11.033.

Barringer, D.M., 1905, Coon Mountain and its crater: Proceedings Academy of Natural Sciences of Philadelphia, v. 57, p. 861–886, http://www.jstor.org/stable/4063062.

Baudemont, D., and Fedorowich, J., 1996, Structural control of uranium mineralization at the Dominique-Peter deposit, Saskatchewan, Canada: Economic Geology, v. 91, p. 855–874, https://doi.org/10.2113/gsecongeo.91.5.855.

Becker, L., Poreda, R.J., Hunt, A.G., Bunch, T.E., and Rampino, M., 2001, Impact event at the Permian–Triassic boundary: Evidence from extraterrestrial noble gases in fullerenes: Science, v. 291, p. 1530–1533, https://doi.org/10.1126/science.1057243.

Becker, L., Poreda, R.J., Basu, A.R., Pope, K.O., Harrison, T.M., Nicholson, C., and Lasky, R., 2004, Bedout: A possible end-Permian impact crater offshore of northwestern Australia: Science, v. 304, p. 1469–1476, https://doi.org/10.1126/science.1093925.

Birks, J.W., Crutzen, P.J., and Roble, R.G., 2007, Frequent ozone depletion resulting from impacts of asteroids and comets, *in* Bobrowsky, P., and Rickman, H., *eds.*, Comet/Asteroid Impacts and Human Society: Springer, New York, p. 225–245, https://doi.org/10.1007/978-3-540-32711-0_13.

Bobrowsky, P., and Rickman, H., *editors*, 2007, Comet/Asteroid Impacts and Human Society: Springer, New York, 546 p.

Bohor, B.F., Foord, E.E., Modreski, P.J., and Triplehorn, D.M., 1984, Mineralogical evidence for an impact at the Cretaceous–Tertiary Boundary: Science, v. 224, p. 867–869, https://doi.org/10.1126/science.224.4651.867.

Brenan, R.L., Peterson, B.I., and Smith, H.J., 1975, The origin of Red Wing Creek Structure, McKenzie County, North Dakota: Wyoming Geological Association Earth Science Bulletin, v. 8, p. 1–41.

Brown, P.G., and 32 others, 2013, A 500-kiloton airburst over Chelyabinsk and an enhanced hazard from small impactors: Nature, v. 503, p. 238–241, https://doi.org/10.1038/nature12741.

Canup, R.M., 2012, Forming a Moon with an Earth-like composition via a giant impact: Science, v. 338, p. 1052–1055, https://doi.org/10.1126/science.1226073.

Canup, R.M., and Asphaug, E., 2001, Origin of the Moon in a giant impact near the end of the Earth's formation: Nature, v. 412, p. 708–712, https://doi.org/10.1038/35089010.

Carpenter, B.N., and Carlson, R., 1992, The Ames impact crater: Oklahoma Geological Survey, v. 52, p. 208–223.

Cavoise., A.J., Wilde, S.A., Liu, D., Weiblen, P.W., and Valley, J.W., 2004, Internal zoning and U–Th–Pb chemistry of Jack Hills zircons: A mineral record of Archean to Mesoproterozoic (4348–1576 Ma) magmatism: Precambrian Research, v. 135, p. 251–279, https://doi.org/10.1016/j.precamres.2004.09.001.

Chambers, J.E., 2001, Making more terrestrial planets: Icarus, v. 152, p. 205–224, https://doi.org/10.1006/icar.2001.6639.

Chambers, J.E., 2004, Planetary accretion in the inner Solar System: Earth and Planetary Science Letters, v. 223, p. 241–252, https://doi.org/10.1016/j.epsl.2004.04.031.

Chao, E.C.T., Shoemaker, E.M., and Madsen, B.M., 1960, First natural occurrence of coesite: Science, v. 132, p. 220–222, https://doi.org/10.1126/science.132.3421.220.

Chapman, C.R., 2004, The hazard of near-Earth asteroid impacts on Earth: Earth and Planetary Science Letters, v. 222, p. 1–15, https://doi.org/10.1016/j.epsl.2004.03.004.

Cohen, A.S., Burnham, O.M., Hawkesworth, C.J., and Lightfoot, P.C., 2000, Pre-emplacement Re–Os ages for ultramafic inclusions in the sublayer of the Sudbury igneous complex: Chemical Geology, v. 165, p. 37–46, http://dx.doi.org/10.1016/S0009-2451(99)00162-x.

Collins, G.S., Melosh, H.J., Morgan, J.V., and Warner, M.R, 2002, Hydrocode simulations of Chicxulub crater collapse and peak-ring formation: Icarus, v. 157, p. 24–33, https://doi.org/10.1006/Icar.2002.6822.

Collins, G.S., Morgan, J., Barton, P., Christeson, G.L., Gulick, S., Urrutia, J., Warner, M., and Wünnemann, K., 2008, Dynamic modeling suggests terrace zone asymmetry in the Chicxulub crater is caused by target heterogeneity: Earth and Planetary Science Letters, v. 270, p. 221–230, https://doi.org/10.1016/j.epsl.2008.03.032.

Connelly, J.N., and Bizzarro, M., 2016, Lead isotope evidence for a young formation age of the Earth–Moon system: Earth and Planetary Science Letters, v. 452, p. 36–43, https://doi.org/10.1016/j.epsl.2016.07.010.

Ćuk, M., and Stewart, S.T., 2012, Making the Moon from a fast-spinning Earth: A giant impact followed by resonant despinning: Science, v. 338, p. 1047–1052, https://doi.org/10.1126/science.1225542.

De Laubenfels, M.W., 1956, Dinosaur extinction: One more hypothesis: Journal of Paleontology, v. 30, p. 207–212, http://www.jstor.org/stable/1300393.

Dickin, A.P., Richardson, J.M., Crocket, J.H., McNutt, R.H., and Peredery, W.V., 1992, Osmium isotope evidence for a crustal origin of platinum group elements in the Sudbury nickel ore, Ontario, Canada: Geochimica et Cosmochimica Acta, v. 56, p. 3531–3537, https://doi.org/10.1016/0016-7037(92)90396-Z.

Dickin, A.P., Artan, M.A., and Crocket, J.H., 1996, Isotopic evidence for distinct crustal sources of North and South Range ores, Sudbury Igneous Complex: Geochimica et Cosmochimica Acta, v. 60, p. 1605–1613, https://doi.org/10.1016/0016-7037(96)00044-0.

Donofrio, R.R., 1981, Impact craters: Implications for basement hydrocarbon production: Journal of Petroleum Geology, v. 3, p. 279–302, https://doi.org/10.1111/j.1747-5457.1981.tb00931.x.

Donofrio, R.R., 1998, North American impact structures hold giant field potential: Oil and Gas Journal, v. 96, p. 69–83.

Dore, M.H.I., 2007, The economic consequences of disasters due to asteroid and comet impacts, small and large, *in* Bobrowsky, P., and Rickman, H., *eds.*, Comet/Asteroid Impacts and Human Society: Springer, New York, p. 479–493, https://doi.org/10.1007/978-3-540-32711-0_29.

Dressler, B.O., 1984, General geology of the Sudbury area, *in* Pye, E.G., Naldrett, A.J., and Giblin, P.E., *eds.*, The Geology and Ore Deposits of the Sudbury Structure: Ontario Geological Survey Special Paper 1, Toronto, p. 57–82.

Faggart Jr., B.E., Basu, A.R., and Tatsumoto, M., 1985, Origin of the Sudbury Complex by meteoritic impact: Neodymium isotopic evidence: Science, v. 230, p.

436–439, https://doi.org/10.1126/science.230.4724.436.
Farrow, C.E.G., and Lightfoot, P.C., 2002, Sudbury PGE revisited: Toward an integrated model, *in* Cabri, L.I., *ed.*, The Geology, Geochemistry, Mineralogy and Beneficiation of Platinum-Group Elements: Canadian Institute of Mining and Metallurgy, Special Volume 54, Montreal, p. 273–297.
French, B.M., and Short, N.M., *editors*, 1968, Shock Metamorphism of Natural Materials: Mono Book Corp., Baltimore, 644 p.
Frey, H., 1980, Crustal evolution of the early Earth: The role of major impacts: Precambrian Research, v. 10, p. 195–216, https://doi.org/10.1016/0301-9268(80)90012-1.
Frimmel, H.E., Groves, D.I., Kirk, J., Ruiz, J., Chesley, J., and Minter, W.E.L., 2005, The formation and preservation of the Witwatersrand goldfields, the world's largest gold province: Economic Geology, v. 100, p. 769–798.
Ganapathy, R., 1980, A major meteorite impact event on the Earth 65 million years ago: Evidence from the Cretaceous–Tertiary boundary clay: Science, v. 209, p. 921–923, https://doi.org/10.1126/science.209.4459.921.
Gibson, R.L., and Reimold, W.U., 2008, Geology of the Vredefort Impact Structures: A Guide to Sites of Interest: South African Council for Geoscience, Memoir 97, Pretoria, 181 p.
Gibson, R.L., Reimold, W.U., and Stevens, G., 1998, Thermal-metamorphic signature of an impact event in the Vredefort dome, South Africa: Geology, v. 26, p. 787–790, https://doi.org/10.1130/0091-7613(1998)026<0787:TMSOAI>2.3.CO;2.
Glickson, A., Hickman, A., Evans, N.J., Kirkland, C.L., Park, J.-W., Rapp, R., and Romano, S., 2016, A new ~3.46 Ga asteroid impact ejecta unit at Marble Bar, Pilbara craton, Western Australia: A petrologic, microprobe and laser ablation ICPMS study: Precambrian Research, v. 279, p. 103–122, https://doi.org/10.1016/j.precamres.2016.04.003.
Goldin, T.J., and Melosh, H.J., 2009, Self-shielding of thermal radiation by Chicxulub impact ejecta: Firestorm or fizzle?: Geology, v. 37, p. 1135–1138, https://doi.org/10.1130/G30433A.1.
Grajales-Nishimura, J.M., Cedillo-Pardo, E., Rosales-Domíniguez, C., Morán-Zenteno, D.J., Alvarez, W., Claeys, P., Ruíz-Morales, J., García-Hernández, J., Padilla-Avila, P., and Sánchez-Ríos, A., 2000, Chicxulub impact: The origin of reservoir and seal facies in the southeastern Mexico oil fields: Geology, v. 28, p. 307–310, https://doi.org/10.1130/0091-7613(2000)28<307:CITOOR>2.0.CO;2.
Green, D.H., 1972, Archean greenstone belts may include terrestrial equivalents of lunar maria?: Earth and Planetary Science Letters, v. 15, p. 263–270, https://doi.org/10.1016/0012-821X(72)90172-0.
Grieve, R.A.F., 1980, Impact bombardment and its role in proto-continental growth on the early Earth: Precambrian Research, v. 10, p. 217–247, https://doi.org/10.1016/0301-9268(80)90013-3.
Grieve, R.A.F., 1984, The impact cratering rate in recent time: Journal of Geophysical Research, v. 89, p. B403–B408, https://doi.org/10.1029/JB089iS02p0B403.
Grieve, R.A.F., 1997, Extraterrestrial impact events: The record in the rocks and the stratigraphic column: Palaeogeography, Palaeoclimatology, Palaeoecology, v. 132, p. 5–23, https://doi.org/10.1016/S0031-0182(97)00058-8.
Grieve, R.A.F., 2012, Economic deposits at terrestrial impact structures, *in* Osinski, G.R., and Pierazzo, E., *eds.*, Impact Cratering: Processes and Products: John Wiley & Sons, Ltd, Chichester, UK, p. 177–193, https://doi.org/10.1002/9781118447307.ch12.
Grieve, R.A.F., and Cintala, M.J., 1992, An analysis of differential impact melt-crater scaling and implications for the terrestrial impact record: Meteoritics, v. 27, p. 526–538, https://doi.org/10.1111/j.1945-5100.1992.tb01074.x.
Grieve, R.A.F., and Kring, D.A., 2007, The geologic record of destructive impact events on Earth, *in* Bobrowsky, P., and Rickman, H., *eds.*, Comet/Asteroid Impacts and Human Society: Springer, New York, p. 3–24, https://doi.org/10.1007/978-3-540-32711-0_1.
Grieve, R.A.F., and Masaitis, V.L., 1994, The economic potential of terrestrial impact craters: International Geology Review, v. 36, p. 105–151, https://doi.org/10.1080/00206819409465452.
Grieve, R.A.F., Stöffler, D., and Deutsch, A., 1991, The Sudbury structure: Controversial or misunderstood?: Journal of Geophysical Research, v. 96, p. 22753–22764, https://doi.org/10.1029/91JE02513.
Grieve, R.A.F., Cintala, M.J., and Therriault, A.M., 2006, Large-scale impacts and the evolution of the Earth's crust: The early years, *in* Reimold, W.U., and Gibson, R.L., *eds.*, Processes on the Early Earth: Geological Society of America Special Papers, v. 405, p. 23–31, https://doi.org/10.1130/2006.2405(02).
Grieve, R.A.F., Reimold, W.U., Morgan, J., Riller, U., and Pilkington, M., 2008, Observations and interpretations at Vredefort, Sudbury and Chicxulub: Towards an empirical model of terrestrial impact basin formation: Meteoritics and Planetary Science, v. 43, p. 855–882, https://doi.org/10.1111/j.1945-5100.2008.tb01086.x.
Hanley, J.J., Mungall, J.E., Pettke, T., Spooner, E.T.C., and Bray, C.J., 2005, Ore metal redistribution by hydrocarbon-brine and hydrocarbon-halide melt phases, North Range footwall of the Sudbury Igneous Complex, Ontario, Canada: Mineralium Deposita, v. 40, p. 237–256, https://doi.org/10.1007/s00126-005-0004-z.
Harrison, T.M., 2009, The Hadean crust: Evidence from > 4 Ga zircons: Annual Review of Earth and Planetary Sciences, v. 37, p. 479–505, https://doi.org/10.1146/annurev.earth.031208.100151.
Hartmann, W.K., and Davis, D.R., 1975, Satellite-sized planetesimals and lunar origin: Icarus, v. 24, p. 504–515, https://doi.org/10.1016/0019-1035(75)90070-6.
Hartmann, W.K., Phillips, R.J., and Taylor, G.J., *editors*, 1986, Origin of the Moon: Lunar and Planetary Institute, Houston, 797 p.
Hayward, C.L., Reimold, W.U., Gibson, R.L., and Robb, L.J., 2005, Gold mineralization within the Witwatersrand Basin, South Africa: Evidence for a modified placer origin, and the role of the Vredefort impact event, *in* McDonald, I.M., Boyce, A.J., Butler, I.B., Herrington, R.J., and Polya, D.A., *eds.*, Mineral Deposits and Earth Evolution: Geological Society, London, Special Publications, v. 248, p. 31–58, http://dx.doi.org/10.1114/GSL.SP.2005.2.48.01.02.
Head, J.W., 2010, Transition from complex craters to multi-ringed basins on terrestrial planetary bodies: Scale-dependent role of expanding melt cavity and progressive interaction with the displaced zone: Geophysical Research Letters, v. 37, L02203, https://doi.org/10.1029/2009GL041790.
Henkel, H., and Reimold, W.U., 1998, Integrated geophysical modelling of a giant, complex impact structure: Anatomy of the Vredefort Structure, South Africa: Tectonophysics, v. 287, p. 1–20, https://doi.org/10.1016/S0040-1951(98)80058-9.
Hildebrand, A.R., Penfield, G.T., Kring D.A., Pilkington, M., Camargo, Z.A., Jacobsen, S.B., and Boynton, W.V., 1991, Chicxulub Crater: A possible Cretaceous/Tertiary boundary impact crater on the Yucatán Peninsula, Mexico: Geology, v. 19, p. 867–871, https://doi.org/10.1130/0091-7613(1991)019<0867:CCAPCT>2.3.CO;2.
Hills, J.G., Nemchinov, I.V., Popov, S.P., and Teterev, A.V., 1994, Tsunami generated by small impacts, *in* Geherls, T., *ed.*, Hazards from comets and asteroids: University Arizona Press, Tucson, p. 779–789.
Hopkins, M., Harrison, T.M., and Manning, C.E., 2008, Low heat flow inferred from > 4 Gyr zircons suggests Hadean plate boundary interactions: Nature, v. 456, p. 493–496, https://doi.org/10.1038/nature07465.
Ivanov, B.A., 2005, Numerical modeling of the largest terrestrial meteorite craters: Solar System Research, v. 39, p. 381–409, https://doi.org/10.1007/s11208-005-0051-0.
Jackson, J.C., Horton, J.W., Chou, I.-M., and Belkin, H.E., 2006, A shock-induced polymorph of anatase and rutile from the Chesapeake Bay impact structure, Virginia, U.S.A.: American Mineralogist, v. 91, p. 604–608, https://doi.org/10.2138/am.2006.2061.
Jaupart, C., and Tait, S., 1995, Dynamics of differentiation in magma reservoirs: Journal of Geophysical Research, v. 100, p. 17615–17636, https://doi.org/10.1029/95JB01239.
Jefferson, C.W., and Delaney, G., *editors*, 2007, EXTECH IV: Geology and uranium exploration technology of the Proterozoic Athabasca Basin, Saskatchewan and Alberta: Geological Association of Canada, Mineral Deposits Division, Special Publication 4, St. John's, NL, 645 p.
Johnson, K.S., and Campbell, J.A., *editors*, 1997, Ames Structure in Northwest Oklahoma and Similar Features: Origin and Petroleum Production: Oklahoma Geological Survey, Circular 100, Norman, 396 p.
Kamo, S.L., Reimold, W.U., Krogh, T.E., and Colliston, W.P., 1996, A 2.023 Ga age for the Vredefort impact event and a first report of shock metamorphosed zircons in pseudotachylitic breccias and granophyre: Earth and Planetary Science Letters, v. 144, p. 369–387, https://doi.org/10.1016/S0012-821X(96)00180-X.
Keller, G., Adatte, T., Pardo, A., Bajpai, S., Khosla, A., and Samant, B., 2010, Cretaceous Extinctions: Evidence overlooked: Science, v. 328, p. 974–975, https://doi.org/10.1126/science.328.5981.974-a.
Kenney, G.G., Whitehouse, M.J., and Kamber, B.S., 2016, Differentiated impact melt sheets may be a potential source of Hadean detrital zircon: Geology, v. 44, p. 435–438, https://doi.org/10.1130/G37898.1.
Kent, D.V., Creamer, B.S., Lanci, L., Wang, D., Wright, J.D., and Van der Voo, R., 2003, A case for a comet impact trigger for the Paleocene/Eocene thermal maximum and carbon isotope excursion: Earth and Planetary Science Letters, v. 211, p. 13–26, https://doi.org/10.1016/S0012-821X(03)00188-2.
Kring, D.A., 2004, Environmental consequences of impact cratering events as a function of ambient conditions on Earth: Astrobiology, v. 3, p. 133–152, https://doi.org/10.1089/153110703321632471.
Kring, D.A., 2007, The Chicxulub impact event and its environmental consequences at the Cretaceous–Tertiary boundary: Palaeogeography, Palaeoclimatology,

Palaeoecology, v. 255, p. 4–21, https://doi.org/10.1016/j.palaeo.2007.02.037.

Kring, D.A., and Durda, D.D., 2002, Trajectories and distribution of material ejected from the Chicxulub impact crater: Implications for post-impact wildfires: Journal of Geophysical Research, v. 107, p. 6-1–6-22, https://doi.org/10.1029/2001JE001532.

Kyte, F.T., Shukolyukov, A., Lugmair, G.W., Lowe, D.R., and Byerly, G.R., 2003, Early Archean spherule beds: Chromium isotopes confirm origin through multiple impacts of projectiles of carbonaceous chondrite type: Geology, v. 31, p. 283–286, https://doi.org/10.1130/0091-7613(2003)031<0283:EASBCI>2.0.CO;2.

Lainé, R., Alonso, D., and Svab, M., *editors*, 1985, The Carswell Structure Uranium Deposits, Saskatchewan: Geological Association of Canada, Special Paper 29, St. John's, NL, 230 p.

Lightfoot, P.C., Keays, R.R., Morrison, G.G., Bite, A., and Farrel, K.P., 1997, Geochemical relationships in the Sudbury Igneous Complex: Origin of the main mass and offset dikes: Economic Geology, v. 92, p. 289–307, https://doi.org/10.2113/gsecongeo.92.3.289.

Lowe, D.R., Byerly, G.R., and Kyte, F.T., 2014, Recently discovered 3.42–3.23 Ga impact layers, Barberton Belt, South Africa: 3.8 Ga detrital zircons, Archean impact history, and tectonic implications: Geology, v. 42, p. 747–750, https://doi.org/10.1130/G35743.1.

MacCracken, M.C., 2007, The climatic effects of asteroid and comet impacts: Consequences for an increasingly interconnected society, *in* Bobrowsky, P., and Rickman, H., *eds*., Comet/Asteroid Impacts and Human Society: Springer, New York, p. 277–289, https://doi.org/10.1007/978-3-540-32711-0_16.

Marchi, S., Bottke, W.F., Elkins-Tanton, L.T., Bierhaus, M., Wuennemann, K., Morbidelli, A., and Kring, D.A., 2014, Widespread mixing and burial of Earth's Hadean crust by asteroid impacts: Nature, v. 511, p. 578–582, https://doi.org/10.1038/nature13539.

Masaitis, V.L., 1998, Popigai crater: Origin and distribution of diamond-bearing impactites: Meteoritics and Planetary Science, v. 33, p. 349–359, https://doi.org/10.1111/j.1945-5100.1998.tb01639.x.

McCarthy, T.S., Stanistreet, I.G., and Robb, L.J., 1990, Geological studies related to the origin of the Witwatersrand Basin and its mineralization: An introduction and a strategy for research and exploration: South African Journal of Geology, v. 93, p. 1–4.

Meier, D.L., Heinrich, C.A., and Watts, M.A., 2009, Mafic dikes displacing Witwatersrand gold reefs: Evidence against metamorphic-hydrothermal ore formation: Geology, v. 37, p. 607–610, https://doi.org/10.1130/G25657A.1.

Melosh, H.J., 1989, Impact Cratering: A Geologic Process: Oxford University Press, New York, 245 p.

Melosh, H.J., 2007, Physical effects of comet and asteroid impacts: Beyond the crater rim, *in* Bobrowsky, P., and Rickman, H., *eds*., Comet/Asteroid Impacts and Human Society: Springer, New York, p. 211–224, https://doi.org/10.1007/978-3-540-32711-0_12.

Melosh, H.J., and Vickery, A.M., 1989, Impact erosion of the primordial atmosphere of Mars: Nature, v. 338, p. 487–489, https://doi.org/10.1038/338487a0.

Melosh, H.J., Schneider, N.M., Zahnle, K.J., and Latham, D., 1990, Ignition of global wildfires at the Cretaceous/Tertiary boundary: Nature, v. 343, p. 251–254, https://doi.org/10.1038/343251a0.

Molnár, F., Watkinson, D.H., and Jones, P.C., 2001, Multiple hydrothermal processes in footwall units of the North Range, Sudbury Igneous Complex, Canada, and implications for the genesis of vein-type Cu–Ni–PGE deposits: Economic Geology, v. 96, p. 1645–1670, https://doi.org/10.2113/gsecongeo.96.7.1645.

Morgan, J., Warner, M., and the Chicxulub Working Group, 1997, Size and morphology of the Chicxulub impact crater: Nature, v. 390, p. 472–476, https://doi.org/10.1038/37291.

Morgan, J.V., Warner, M.R., Collins, G.S., Grieve, R.A.F., Christeson, G.L., Gulick, S.P.S., and Barton, P.J., 2011, Full waveform tomographic images of the peak ring at the Chicxulub impact crater: Journal of Geophysical Research, v. 116, B06303, https://doi.org/10.1029/2010JB008015.

Morgan, J.V., Artemieva, N., and Goldin, T., 2013, Revisiting wildfires at the K–Pg boundary: Journal of Geophysical Research, v. 118, p. 1508–1520, https://doi.org/10.1002/2013JG002428.

Morgan, J.V., Gulick, S.P.S., Urrutia-Fucugauchi, J., Collins, G.S., Perz-Cruz, L., and Rebolledo-Vieyra, M., 2015, IODP-ICDP expedition 364: Drilling the K–Pg impact structure (Abstract): Lunar and Planetary Science Conference 46, #1747.

Morgan, J.V., and 38 others, 2016, The formation of peak rings in large impact craters: Science, v. 354, p. 878–882, https://doi.org/10.1126/science.aah6561.

Morgan, J.W., Walker, R.J., Horan, M.F., Beary, E.S., and Naldrett, A.J., 2002, ^{190}Pt–^{186}Os and ^{187}Re–^{187}Os systematics of the Sudbury Igneous Complex, Ontario: Geochimica et Cosmochimica Acta, v. 66, p. 273–290, https://doi.org/10.1016/S0016-7037(01)00768-2.

Naldrett, A.J., 2003, From impact to riches: Evolution of geological understanding as seen at Sudbury: GSA Today, v. 13, p. 4–9.

Neukum, G., and Ivanov, B.A., 1994, Crater size distributions and impact probabilities on Earth from lunar, terrestrial-planet and asteroidal cratering data, *in* Geherels, T., *ed*., Hazards due to Comets and Asteroids: University of Arizona Press, Tucson, p. 359–416.

Officer, C.B., Hallam, A., Drake, C.L., and Devine, J.D., 1987, Late Cretaceous and paroxysmal Cretaceous/Tertiary extinctions: Nature, v. 326, p. 143–149, https://doi.org/10.1038/326143a0.

Osinski, G.R., and Kring, D.A., *editors*, 2015, Large Meteorite Impacts and Planetary Evolution V: Geological Society of America Special Papers, v. 518, 227 p., https://doi.org/10.1130/9780813725185.

Osinski, G.R., and Pierazzo, E., *editors*, 2012, Impact Cratering: Processes and Products: John Wiley & Sons, Ltd, Chichester, UK, 336 p., https://doi.org/10.1002/9781118447307.

Penfield, G.T., and Camargo, A.Z., 1981, Definition of a major igneous zone in the central Yucatan platform with aeromagnetic and gravity (Abstract): Society of Exploration Geophysists, 51st Annual International Meeting, Houston.

Pierazzo, E., Kring, D.A., and Melosh, H.J., 1998, Hydrocode simulation of the Chicxulub impact event and the production of climatically active gases: Journal of Geophysical Research, v. 103, p. 28607–28625, https://doi.org/10.1029/98JE02496.

Pope, K.O., 2002, Impact dust not the cause of the Cretaceous–Tertiary mass extinction: Geology, v. 30, p. 99–102, https://doi.org/10.1130/0091-7613(2002)030<0099:IDNTCO>2.0.CO;2.

Pope, K.O., Baines, K.H., Ocampo, A.C., and Ivanov, B.A., 1994, Impact winter and the Cretaceous/Tertiary extinctions: Results of a Chicxulub asteroid impact model: Earth and Planetary Science Letters, v. 128, p. 719–725, https://doi.org/10.1016/0012-821X(94)90186-4.

Pope, K.O., Baines, K.H., Ocampo, A.C., and Ivanov, B.A., 1997, Energy, volatile production, and climatic effects of the Chicxulub Cretaceous/Tertiarty impact: Journal of Geophysical Research, v. 102, p. 21645–21664, https://doi.org/10.1029/97JE01743.

Rasmussen, B., and Koeberl, C., 2004, Iridium anomalies and shocked quartz in a Late Archean spherule layer from Pilbara craton: New evidence for a major asteroid impact at 2.63 Ga: Geology, v. 32, p. 1029–1032, https://doi.org/10.1130/G20825.1.

Reimold, W.U., Köber, C., Fletcher P., Killick, A.M., and Wilson, J.D., 1999, Pseudotachylitic breccias from fault zones in the Witwatersrand Basin, South Africa: Evidence of autometasomatism and post-brecciation alteration processes: Mineralogy and Petrology, v. 66, p. 25–53, https://doi.org/10.1007/BF01161721.

Reimold, W.U., Koeberl, C., Gibson, R.L., and Dressler, B.O., 2005, Economic mineral deposits in impact structures: A review, *in* Koeberl, C., and Henkel, H., *eds*., Impact Tectonics: Springer, Heidelberg, p. 479–552, https://doi.org/10.1007/3-540-27548-7_20.

Robb, L.J., and Robb, V.M., 1998, Gold in the Witwatersrand Basin, *in* Wilson, M.G.C., and Anhaeusser, C.R., *eds*., The Mineral Resources of South Africa: Geoscience Council of South Africa, Handbook 16, Pretoria, p. 294–349.

Robertson, D.S., Lewis, W.M., Sheehan, P.M., and Toon, O.B., 2013, K–Pg extinction: Reevaluation of the heat-fire hypothesis: Journal of Geophysical Research, v. 118, p. 329–336, https://doi.org/10.1002/jgrg/20018.

Santiago-Acevedo, J., 1980, Giant fields of the southern zone-Mexico, *in* Halbouty, M.T., *ed*., Giant Oil and Gas Fields of the Decade 1968–1978: American Association of Petroleum Geologists, Memoir 30, Tulsa, p. 339–385.

Sawatzky, H.B., 1977, Buried impact structures in the Williston Basin and adjacent area, *in* Roddy, D.J., Pepin, R.O., and Merrill, R.B., *eds*., Impact and Explosion Cratering: Pergamon, New York, p. 461–480.

Schaller, M.F., Fung, M.K., Wright, J.D., Katz, M.E., and Kent, D.V., 2016, Impact ejecta at the Paleocene–Eocene boundary: Science, v. 354, p. 225–229, https://doi.org/10.1126/science.aaf5466.

Schulte, P., and 40 others, 2010, The Chicxulub asteroid impact and mass extinction at the Cretaceous–Paleogene boundary: Science, v. 327, p. 1214–1218, https://doi.org/10.1126/science.1177265.

Scott, R.G., and Spray, J.G., 2000, The South Range breccia belt of the Sudbury impact structure; a possible terrace collapse feature: Meteoritics and Planetary Science, v. 35, p. 505–520, https://doi.org/10.1111/j.1945-5100.2000.tb01432.x.

Sharpton, V.L., Marín, L.E., Carney, J.L., Lee, S., Ryder, G., Schuraytz, B.C., Sikora, P., and Spudis, P.D., 1996, A model of the Chicxulub impact basin based on evaluation of geophysical data, well logs, and drill core samples, *in* Ryder, G., Fastovsky, D.E., and Gartner, S., *eds*., The Cretaceous–Tertiary Event and Other Catastrophes in Earth History: Geological Society of America Special Papers,

v. 307, p. 55–74, https://doi.org/10.1130/0-8137-2307-8.55.

Shuvalov, V.V., and Artemieva, N.A., 2002, Atmospheric erosion and radiation impulse induced by impacts, *in* Koeberl, C., and Macleod, K.G., *eds.*, Catastrophic Events and Mass Extinctions: Impacts and Beyond: Geological Society of America Special Papers, v. 356, p. 695–703, https://doi.org/10.1130/0-8137-2356-6.695.

Simonson, B.M., and Glass, B.P., 2004, Spherule layers–records of ancient impacts: Annual Review of Earth and Planetary Science, v. 32, p. 329–361, https://doi.org/10.1146/annurev.earth.32.101802.120458.

Simonson, B.M., Sumner, D.Y., Beukes, N.J., Johnson, S., and Gutzmer, J., 2009, Correlating multiple Neoarchean–Paleoproterozoic impact spherule layers between South Africa and Western Australia: Precambrian Research, v. 169, p. 100–111, https://doi.org/10.1016/j.precamres.2008.10.016.

Smith, F.C., Glass, B.P., Simonson, B.M., Smith, J.P., Krull-Davatzes, A.E., and Booksh, K.S., 2016, Shock-metamorphosed rutile grains containing the high pressure polymorph TiO_2-II in four Neoarchean spherule layers: Geology, v. 44, p. 775–778, https://doi.org/10.1130/G38327.1.

Stöffler, D., Deutsch, A., Avermann, A., Bischoff, L., Brockmeyer, P., Buhl, D., Lakomv, R., and Müller-Mohr, V., 1994, The formation of the Sudbury Structure, Canada: Toward a unified impact model, *in* Dressler, B.O., Grieve, R.A.F., and Sharpton, V.L., *eds.*, Large Meteorite Impacts and Planetary Evolution: Geological Society of America Special Papers, v. 293, p. 303–318, https://doi.org/10.1130/SPE293-p303.

Stöffler, D., Ryder, G., Ivanov, B.A., Artemieva, N.A., Cintala, M.J., and Grieve, R.A.F., 2006, Cratering history and lunar chronology: Reviews in Mineralogy and Geochemistry, v. 60, p. 519–596, https://doi.org/10.2138/rmg.2006.60.05.

Therriault, A.M., Grieve, R.A.F., and Reimold, W.U., 1997, Original size of the Vredefort structure: Implications for the geological evolution of the Witwatersrand Basin: Meteoritics and Planetary Science, v. 32, p. 71–77, https://doi.org/10.1111/j.1945-5100.1997.tb01242.x.

Therriault, A.M., Fowler, A.D., and Grieve, R.A.F., 2002, The Sudbury Igneous Complex: A differentiated impact melt sheet: Economic Geology, v. 97, p. 1521–1540, https://doi.org/10.2113/gsecongeo.97.7.1521.

Thomas, P.J., Hicks, R.D., Chyba, C.F., and McKay, C.P., *editors*, 1997, Comets and the Origin Evolution of Life: Springer, Berlin, 357 p., https://doi.org/10.1007/10903490.

Toon, O.B., Zahnle, K., Morrison, D., Turco, R.P., and Covey, C., 1997, Environmental perturbations caused by the impact of asteroids and comets: Reviews of Geophysics, v. 35, p. 41–78, https://doi.org/10.1029/96RG03038.

Tuchscherer, M.G., and Spray, J.G., 2002, Geology, mineralization and emplacement of the Foy offset dike, Sudbury impact structure: Economic Geology, v. 97, p. 1377–1398, https://doi.org/10.2113/gsecongeo.97.7.1377.

Tucker, R.T., Viljoen, R.P., and Viljoen, M.J., 2016, A review of the Witwatersrand Basin–the world's greatest goldfield: Episodes, v. 39, p. 105–133, https://doi.org/10.18814/epiiugs/2016/v39i2/95771.

Vellekoop, J., Esmeray-Senlet, S., Miller, K.G., Browning, J.V., Sluijs, A., van de Schootbrugge, B., Sinninghe Damsté, J.S., and Brinkhuis, H., 2016, Evidence for Cretaceous–Paleogene boundary bolide "impact winter" conditions from New Jersey, USA: Geology, v. 44, p. 619–622, https://doi.org/10.1130/G37961.1.

Vonhof, H.B., Smit, J., Brinkhuis, H., Montanari, A., and Nederbragt, A.J., 2000, Global cooling accelerated by early late Eocene impacts?: Geology, v. 28, p. 687–690, https://doi.org/10.1130/0091-7613(2000)28<687:GCABEL>2.0.CO;2.

Walkden, G., Parker, J., and Kelley, S., 2002, A late Triassic impact ejecta layer in southwestern Britain: Science, v. 298, p. 2185–2188, https://doi.org/10.1126/science.1076249.

Walker, R.J., Morgan, J.W., Naldrett, A.J., Li, C., and Fassett, J.D., 1991, Re–Os isotope systematics of Ni–Cu sulphide ores, Sudbury Igneous Complex, Ontario: Evidence for a major crustal component: Earth and Planetary Science Letters, v. 105, p. 416–429, https://doi.org/10.1016/0012-821X(91)90182-H.

Ward, P.L., 2009, Sulfur dioxide initiates global climate change in four ways: Thin Solid Films, v. 517, p. 3188–3203, https://doi.org/10.1016/j.tsf.2009.01.005.

Warner, S., Martin, R.F., Abdel-Raham, A.F.M., and Doig, R., 1998, Apatite as a monitor of fractionation, degassing and metamorphism in the Sudbury Igneous Complex, Ontario: Canadian Mineralogist, v. 36, p. 981–999.

Watson, E.B., and Harrison, T.M., 2005, Zircon thermometer reveals minimum melting conditions on earliest Earth: Science, v. 308, p. 841–844, https://doi.org/10.1126/science.1110873.

Wiechert, U., Halliday, A.N., Lee, D.-C., Snyder, G.A., Taylor, L.A., and Rumble, D., 2001, Oxygen isotopes and the moon-forming giant impact: Science, v. 294, p. 345–348, https://doi.org/10.1126/science.1063037.

Wielicki, M.M., Harrison, T.M., and Schmitt, A.K., 2012, Geochemical signature and magmatic stability of terrestrial impact produced zircons: Earth and Planetary Science Letters, v. 321–322, p. 20–31, https://doi.org/10.1016/j.epsl.2012.01.009.

Woolbach, W.S., Gilmour, I., and Anders, E., 1990, Major wildfires at the Cretaceous/Tertiary boundary, *in* Sharpton, V.L., and Ward, P.D., *eds.*, Global Catastrophes in Earth History: An Interdisciplinary Conference on Impacts, Volcanism, and Mass Mortality: Geological Society of America Special Papers, v. 247, p. 391–400, https://doi.org/10.1130/SPE247-p391.

Zahnle, K.J., and Sleep, N.H., 1997, Impacts and the early evolution of life, *in* Thomas, P.J., Chyba, C.F., and McKay, C.P., *eds.*, Comets and the Origin of Life: Springer-Verlag, New York, p. 175–208, https://doi.org/10.1007/978-1-4757-2688-6_8.

Zhang, J., Dauphas, N., Davis, A.M., Leya, I., and Fedkin, A., 2012, The proto-Earth as a significant source of lunar material: Nature Geoscience, v. 5, p. 251–255, https://doi.org/10.1038/ngeo1429.

Zhao, B., Robb, L.J., Harris, C., and Jordaan, L.J., 2006, Origin of hydrothermal fluids and gold mineralization associated with the Ventersdorp Contact Reef, Witwatersrand Basin, South Africa: Constraints from S, O, and H isotopes, *in* Reimold, W.U., and Gibson, R.L., *eds.*, Processes on the Early Earth: Geological Society of America Special Papers, v. 405, p. 333–352, https://doi.org/10.1130/2006.2405(17).

Received November 2016
Accepted as revised January 2017
First published on the web February 2017